PONTIFICIA UNIVERSIDAD CATOLICA DE CHILE
ESCUELA DE INGENIERIA

THERMODYNAMIC EFFICIENCY OF A COPPER COMMINUTION PROCESS

WILHELM ALEXANDER JACOB RODRÍGUEZ

Thesis submitted to the Office of Research and Graduate Studies in partial fulfillment of the requirements for the Degree of Master of Science in Engineering

Advisor:

PHD. JORGE RAMOS GREZ

Santiago de Chile, August, 2016

© MMXVI año, Wilhelm Alexander Jacob Rodríguez

PONTIFICIA UNIVERSIDAD CATOLICA DE CHILE

ESCUELA DE INGENIERIA

THERMODYNAMIC EFFICIENCY OF A COPPER COMMINUTION PROCESS

WILHELM ALEXANDER JACOB RODRIGUEZ

Members of the Committee:

PHD. JORGE RAMOS GREZ

PHD. WOLFRAM JAHN

PHD .TIMOTHY GUTOWSKI

PHD. ANGEL ABUSLEME

Thesis submitted to the Office of Research and Graduate Studies in partial fulfillment of the requirements for the Degree of Master of Science in Engineering

Santiago de Chile, August 2016

To my parents, siblings and girlfriend whom all, in their own way, showed their support during the development of this work. To Professor Ramos whom presented this great opportunity and guided throughout its study. To Dan and Tim who patiently coached and helped during this study.

ACKNOWLEDGEMENTS

To God almighty whom I owe everything I am, his blessing for having a privileged education and health, loving family and girlfriend and good friends. May he forever guide my path and that this work be of contribution for others, for their wellbeing and his glory.

To my parents, whom I owe my whole lifetime education, love and support. To my father who gave me practical counsel, to my mother who gave me all the help she could give me. To my siblings whom, in their own way, helped and supported me during this project.

Special thanks to my loving girlfriend who had my back in difficult times. To have heard and counseled me on different aspects, stood by my side and light my days with joy and love during the whole development of this thesis.

Professor Ramos whom presented this great opportunity and with a guiding patience, supervised and helped to develop this thesis.

To Dan who coached, corrected and helped on the development of the theory and paper travelling all the way here twice and also hosted my visit to the MIT campus.

To Tim who travelled, gave the time and worked great distances to make this possible.

To the whole mechanical engineering staff whom assisted with the laboratory experiments, especially Professor Perez who patiently counseled on the various details of the laboratory experiment and assisted on measuring several parameters.

To every teacher, faculty member, student and fellow colleague who've I met and helped me during my professional education and to those who've taught me valuable life lessons during my career with or without their knowledge on doing so.

And of course I am greatly thankful to the Misti Fund and the Minera San Pedro, to whom with their funding, samples and disposition made this whole research possible.

GENERAL INDEX

Page

TABLE INDEX

Page

TABLE OF FIGURES

Page

ABSTRACT

This study analyzes the exergy efficiency of comminution in a copper mining plant in the central region of Chile. The development of the analysis was made using a laboratory sized dry ball mill and uniaxial compression to obtain the theoretical and practical minimum work for comminution based on the Hukki-Morell relationship and minimum machinery energy estimations. The energy requirements of comminution are traditionally predicted using the Bond work index. However, it does not provide a benchmark for calculating the crushing and grinding comminution efficiency. This new minimum work index was first used to analyze the efficiency of comminution of the laboratory dry ball mill at different rpms and operations times, as to apply the modeling and data obtained to analyze and compare with a larger wet ball mill and crushing machinery. An exergy analysis was calculated for a laboratory sized dry ball mill by considering the Hukki and Morrell combined relationships, the minimum machinery energy, and the surface energy difference between large and small rocks. It was found that the surface energy analysis, although a closer representation of the thermodynamic efficiency, suggests that impractical improvements to the comminution process are possible. Therefore, it was concluded that the efficiency calculated using a compression tests and a Hukki-Morrell relationship is a better efficiency measure for comparing comminution techniques and machinery inertial calculations for comparing the machine of a same type such as comparing ball mills. Although only for certain size ranges from which machinery capacity to produce the grain size comes into play. Furthermore, efficiency obtained from an exergy analysis of the dry and wet ball milling process and the mining plant comminution equipment verified the usefulness of the Hukki-Morrell relationship and suggests that the efficiency is of the order of 2.97%, 16.6% and 31.7% respectively. Through analyzing our experimental equipment and the machinery of the mine, it was found that the machinery inertial efficiency is of an average 21.32% for our dry ball mill, 84.04% for the wet ball mill and 64.4% in average for the mining plant comminution equipment. Moreover, the majority of the energy leaves as heat losses through friction in the transmission system of the mill and, for the crushers, through the shell and refrigerant system. One could also, theoretically, use the low temperature heat from the outgoing crushed material to perform work, but even this would only increase the efficiency to 3.08%, 19.3% and 34.8% respectively. Additionally, electrical energy measurements and machinery calculations on operating an empty versus loaded ball mill suggest that the efficiency could be increased by ensuring correct machinery scaling, steel ball load and well maintained transmission system. A graph was also developed to define operational ranges for constant grain size difference (between incoming and outgoing rocks), energy and efficiency for the laboratory mill.

Keywords: COMMINUTION; EXERGY; BALL MILL, MINIMUM WORK ENERGY;

RESUMEN

Este estudio analiza la eficiencia exergética de una planta minera de cobre de una región central de Chile. El desarrollo del análisis usado fue basado en un molino de bolas en seco de laboratorio y un equipo de compresión uniaxial para obtener el mínimo teórico y práctico para conminución basado en la relación de Hukki-Morrell y en estimaciones de energía mínima de maquinaria. Tradicionalmente, los requerimientos de energía para conminución son establecidas utilizando el índice de trabajo de Bond. Sin embargo, éste no provee un punto de referencia suficientemente apto para calcular eficiencia para conminución de molienda y chancado. Este nuevo trabajo mínimo fue utilizado en primera instancia para analizar la eficiencia para conminución de un molino de bolas de laboratorio a diferentes rpm y tiempos de operación, para luego aplicar el modelo y datos obtenidos para analizar y comparar el proceso a un molino de bolas húmedo y maquinaria de chancado. Un análisis de exergía fue calculado para el molino de bolas en seco de laboratorio considerando una relación combinada de Hukki-Morrell, energía mínima de maquinaria y diferencia de energía de superficie entre rocas grandes y pequeñas. Fue encontrado que el análisis de energía de superficie, aunque sea una representación más cercana de la eficiencia termodinámica, sugiere que mejoramientos imprácticos son posibles para mejorar el proceso. De tal forma, fue concluido que la eficiencia calculada utilizando compresión uniaxial y una relación Hukki y Morrell es una mejor medida para comparar técnicas de conminución y cálculos inerciales de maquinaria para comparar maquinaria del mismo tipo como por ejemplo molinos de bolas. Aunque esto solo para ciertos rangos de tamaño en donde la capacidad de la maquinaria para producir el tamaño

de partícula comienza a tomar protagonismo. Además, la eficiencia obtenida de un análisis exergético de un molino de bolas húmedo, en seco y de los equipos de conminución de la planta verifican la utilidad de una relación Hukki-Morrell y sugieren que la eficiencia es del orden de 2.97%, 16.6% y 31.7% respectivamente. Al analizar nuestra maquinaria experimental de laboratorio y la de la planta minera, fue encontrado que la eficiencia inercial de la maquinaria es en promedio de un 21.32% para el molino de bolas en seco del laboratorio, 84.04% para el molino de bolas en húmedo y de un 64.4% en promedio para la maquinaria de conminución de la planta. Además, la mayoría de la energía sale como pérdidas de calor por el sistema de transmisión y, para las chancadoras, por la carcasa y el aceite refrigerante. Uno podría, teóricamente, utilizar este calor de baja temperatura del material para realizar trabajo, aunque incluso esto solo incrementaría la eficiencia a un 3.08%, 19.3% y un 34.8% respectivamente. Adicionalmente en el molino de bolas en seco de laboratorio, mediciones de energía eléctrica y cálculos de maquinaria operando vacío y con carga de bolas sugiere que la eficiencia puede ser incrementada por asegurarse un correcto escalamiento de la maquinaria, carga de bolas y un sistema de transmisión bien mantenido. También, un gráfico fue desarrollado para definir rangos de operación para tamaños de grano constante, energía y eficiencia energética para el molino de bolas en seco de laboratorio.

1. INTRODUCTION

In 2014, the copper mining industry in Chile consumed nearly 161,716 TJ of electrical energy with an annual increment of 4.4% from 2013 (Comisión Chilena del Cobre, 2015). According to the Chilean National Institute of Energy, in 2010, the Chilean mining industry was responsible for 34.9% of the total energy consumed nationwide (Instituto Nacional de Estadísticas Chile, 2013). Besides the high energy consumption, the mining industry unfortunately also produces excessive amounts, of approximately 700-800 thousand ton per year, of toxic tailings and wastes (SERNAGEOMIN Chile, 2015). This makes an interesting case for research for anyone who is into sustainable production and optimizing environmental impact.

The copper mining and processing can be summarized into five phases: (i) Mining and extraction of the copper ore; (ii) crushing; (iii) fine grinding; (iv) flotation/lixiviation (or, in other words, separation of copper from the gangue, the remainder of the mined material); and (v) smelting. The third and fifth phases are the most energy consuming phases, representing approximately 90% of the total energy of the process (United States Geological Survey, 2011). In Chile, smelting is outsourced to foreign countries due to the high local cost of energy. Therefore, in Chile, fine grinding is the main aim for most energy efficiency assessments in copper mining.

In this study, we shall review the San Pedro Mining facility, a copper mine in a central region of Chile (Til Til) which counts with the capacity of performing digging and extracting operations from the nearby mines; crushing machinery which consists on a primary jaw crusher and a secondary and tertiary cone crushers; wet ball mill fine grinding; and a final concentration phase of flotation with a Rougher, Cleaner and Scavenger followed by a final drying process. This results in a copper concentrate which is later sold for exportation to be smelted.

For the assessment of the efficiency of the crushing and grinding of a copper ore, an experimental dry ball mill setup was used so to obtain information for a real case scenario of a mining plant in Chile using the first and second laws of thermodynamics. An exergy rate balance and efficiency calculations based both on inertial calculations and on minimum comminution energy obtained by uniaxial compression tests and a combination of a Hukki and Morrell relationships were developed and later applied with the plant parameters. The results were later illustrated in Sankey and Grassmann diagrams. Sankey diagrams are a type of flow diagram in which the arrows, which commonly represent energy, are illustrated proportionally to the flow quantity. On the other hand, Grassmann diagrams illustrate energy flows with arrows but considers the entropy losses in the process typically illustrated with a triangle subtraction to the arrow. Therefore, the latter diagram is used as to express exergy flows.

In the first Chapter, we shall introduce the assessment of the comminution phases of the plant based on exergy efficiency analysis. On Chapter 2 we show the main article, which contains the exergy assessment on a laboratory sized dry ball mill, so to have a controlled environment as to study different aspects of dry ball mill grinding. This was accomplished utilizing different available comminution relationships to determine the minimum energy required reviewed throughout the Chapter. On Chapter 3, we obtain operational parameters for the laboratory equipment utilizing the data results from the previous chapter. We later compare these results with the data and results obtained with the same material sample obtained for the mining site. In the analysis throughout this study, we will also review if the capture of the heat of the material would be of relevance to consider, and if scaling or other factors could be considered for energy efficiency. In section 3.3 we will state the main conclusions of the study and on 3.4 some proposal ideal for future research.

1.1 Literature Review

1.1.1 Comminution

A general description of comminution can be taken from Gupta as: *"Comminution encompasses all the terms, crushing, grinding and other words of phrases associated with the size reduction or severance of ores and rocky materials"* (Gupta, 2003). A problem usually confronted with this process is the fact that it is a random process. Not only in occurrence from circumstance, but also in geometry, composition of the minerals and the angles in which the rocks are smashed also random. This problem also includes the different mechanisms in which comminution occurs. Furthermore, three mechanisms can be defined: abrasion, cleavage and fracture (Monov, Sokolov, & Stoenchev, 2012). All illustrated in Figure 1-1.

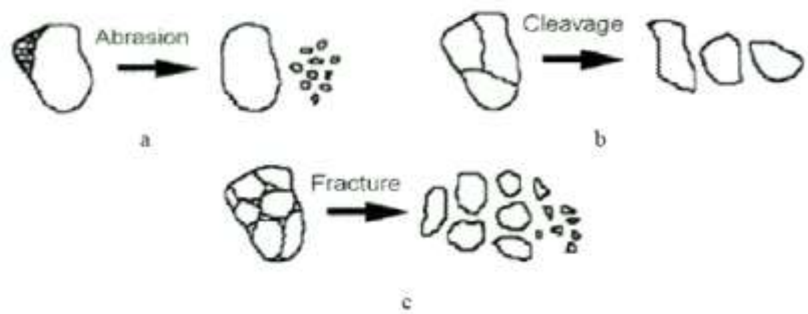

Figure 1-1 Drawing illustrating different mechanisms of comminution (Monov et al., 2012)

These three mechanisms of comminution can be described as: “Abrasion occurs when local low intensity stresses are applied and the result is fine particles taken from the surface of the mother particle and particles of size close to the size of the mother particle. Cleavage of particles occurs when slow and relatively intense stresses are applied (compression) which produce fragments of size 50-80% of the size of the initial particle. Fracture is a result of rapid applications of intense stresses (impact) which produce fragments of relatively small sizes with a relatively wide particle size distribution“ (Monov et al., 2012).

Throughout the years, several researchers have attempted to model the mechanical work needed to break a rock of diameter *x*. The earliest significant work was in 1867 by Rittinger who modeled the energy needed to crush a given size of rock as dependent on its surface area, proportional to x^2 (Rittinger, 1867). Later in the 19th century, Kick modeled the energy required to crush a given size of rock as dependent on its volume

(Kick, 1885). Nearly seventy years then passed before Bond presented his now ubiquitous method for calculating comminution work (Bond, 1952). Bond modeled the energy required to crush a given size of rock as proportional to the geometric mean of surface area and volume area, $x^{5/2}$. In order to calculate the energy required to crush rock from one diameter to another, differential forms of the Rittinger, Kick and Bond models are integrated from x_0 to x_1. Equation (1.1) presents the differential form of these models where *dE* denotes the differential amount of energy needed to reduce the ore size from infinity to a certain size, *x* refers to the evaluated ore size (in µm), *K* is a scaling parameter (in force units) which distinguishes materials ore from one another and is the common characteristic parameter for the material but is not necessarily the same value for different relationships, and *m* is a dimensionless constant which is equal to 2 for Rittinger's, 1 for Kick's, and 1.5 for Bond's models of comminution (see Morrell, (2004) for more details).

$$dE = -K \cdot x^{-m} dx \tag{1.1}$$

In 1962, Hukki noticed that the constant *m* was valid only in certain ore size ranges (Hukki, 1962). Kapur and later on Lynch clarified that the curve described by Hukki, represented in its differential form in Equation (1.2), differs from the previous models in that the exponent, *m*, corresponds to a function *f(x)* taking account of the size, *x*, of the material (Kapur & Fuerstenau, 1987; Lynch, 1977). In Equations (1.1) and (1.2), the exponents *m* and *f(x)* (which are dimensionless) characterize the energy consumption needed to crush the material as its size reduces, porosities commence to capsize and the rock finally becomes dust.

$$dE = -K \cdot x^{-f(x)} dx \tag{1.2}$$

In 2004, Morrell proposed that *K* also varies with ore size through a characteristic variation *C(x)* but maintained a material constant *K'* as shown in Equation (1.3) (Morrell, 2004). The same study goes even further proposing that the exponent function can be represented linearly with parameters a and b as shown in Equation (1.4), both obtained empirically.

$$dE = -K' \cdot C(x) \cdot x^{-f(x)} \tag{1.3}$$

$$f(x) = a + xb \tag{1.4}$$

In this study, we shall maintain the usage of Hukki equation form due to the fact that it is comparable to Bond's equation when using the same materials constant. On the other hand, we shall also test the usefulness of considering the linearity of the exponent, Equation (1.4), for estimating the behavior of the material in other size reduction ranges, as seen in Equation (1.5) .

$$dE = -K \cdot x^{-(a+xb)} dx \tag{1.5}$$

All of these previous comminution relationships studies lead to the notion that industrial calculations for comminution minimum energy are fundamented on semi-empirical correlations based on theoretically reasoned scaling laws. The selection of the semi-empirical correlation and the obtainment of the minimum energy value will be important throughout the course of this study.

1.1.2 Thermodynamics and Exergy

Commonly, engineers analyze plants and processes according to the first thermodynamic law. The first law concerns the conservation of energy, which for a steady state manufacturing process, translates to a balance among all energy flows into and out of the system. In the attempt of defining the minimum energy required, researchers have studied lengths on how to determine this. There are principally four ways to analyze comminution energy: (i) surface energy, (ii) kinetics, (iii) fracture mechanics and (iv) empirical testing (Mular, 1965; Tromans, 2008). The first three are mainly theoretical, hard to define, thoroughly researched and turn difficult when considering the different ore at the different locations of the mine with different concentrations and characteristics. The fourth method is a more practical and most widely used by mining engineers as for project evaluations.

The second law of thermodynamics considers the energy loss due to the irreversibility of the process. This concept, known as *entropy*, was originally introduced by Clausius in 1854 in his work 'The Mechanical Theory of Heat' (Clausius, 1879) . It is a statistical measure of the dispersion of energy, and a quantification of the reversibility of it returning to its original state. In an ideal or reversible process, this value is equal to zero. For a real process, there will be irreversibilities losses of reversibly sub processes, therefore entropy would take a positive or negative value.

This leads to the concept of available work, or exergy, which is equal to the maximum amount of work that can be obtained as a result of a given system coming into equilibrium with a reference state defined by its (constant) temperature, pressure and chemical potentials. Alternatively, exergy may be defined as the minimum work that is needed to create a given system from another system in equilibrium with the reference state. Exergy is not a conserved property, and the more exergy is destroyed, the more irreversible and inefficient the process under consideration. An exergy analysis allows the definition of a benchmark thermodynamic minimum work requirement, which is useful when evaluating efficiencies, and also allows both material and energy flows to be directly compared (Rosen, Dincer, & Kanoglu, 2008). Therefore, adopting an exergy evaluation analysis of the system provides an optimization limit at which the process could not be, theoretically, further improved. A more detailed discussion on exergy, entropy, and the second law of thermodynamics can be found in Bakshi, Gutowski, & Sekulic (2011).

In order to conduct an exergy assessment a reference state is required, because exergy will always depend on differences between the state of the system and environment (Bakshi et al., 2011). This reference state can be defined as being at ambient temperature, T_o, ambient pressure, P_o, and an idealized chemical composition such as that defined by Szargut (Szargut, Morris, & Steward, 1987). In this manner, the exergy definition is given in its differential form by Equation (1.6), where h is enthalpy, s is entropy and T is the actual temperature of the system. Although the expression for the definition of exergy shares some similarity to the Gibbs (Gibbs, 1879) or the Helmholtz (von Helmholtz, 1882) free energy expressions, they are not equivalent due to the temperature reference point T_0, where on the other hand, for Helmholtz/Gibbs free energy corresponds to the substance's temperature *T*. The total exergy of the system (excluding potential and kinetic energy) is typically expressed as the sum of the chemical and the physical exergies, see Equation (1.7).

$$\boldsymbol{dEx = dh(T) - T_0 dS(T)} \tag{1.6}$$

The physical exergy depends on temperature and pressure changes, as shown in Equations (1.6) and (1.8) where, *Cp* is the heat capacity of the material. In this analysis there are no pressure changes.

$$E_{sys} = E_{ch} + E_{ph} \tag{1.7}$$

$$E_{ph} = Cp(T - T_0) - T_0 Cp\, ln\left(\frac{T}{T_0}\right) \tag{1.8}$$

The chemical exergy depends on the bonding energy of the atoms and their configuration that make up the material ore considered and it can be expressed as Equation (1.9).

$$ex_M^{ch} = \sum x_i ex_i^{ch} + R\, T_0 \sum x_i ln(x_i) \tag{1.9}$$

Chemical exergy is therefore obtained by utilizing the known composition of the ore, known exergy values for the different minerals (Szargut et al., 1987) and utilizing Equation (1.9), where ex_M^{ch} is the resulting chemical exergy of the mineral; ex_i^{ch} is the chemical composition of the i^{th} component; x_i is the molar fraction of the component and *R*, the ideal gas constant. Additionally, during this study, we will also consider the surface energy of particles which is to be considered as part of the chemical exergy and comminution (surface energy difference) shall be correlated it as a surface exergy work.

Having this consideration, the general exergy rate balance analysis of an open system is given by Equation (1.10).

$$\dot{E}x_{in} + \dot{E}x_{W} + \dot{E}x_{heatIN} = \dot{E}x_{out} + \dot{E}x_{heatOUT} + \dot{E}x_{des} \tag{1.10}$$

$\dot{E}x_{in}$ and $\dot{E}x_{out}$ considers all incoming and outgoing materials rates through the system, including the objective product as well as wastes and additional manufacturing materials (accounting for the chemical and physical exergies discussed above); $\dot{E}x_{heatIN}$and $\dot{E}x_{heatOUT}$ consider the incoming and outgoing heat flow rates through the system and $\dot{E}x_{des}$ is the destroyed exergy rate of the system. This latter term is the objective function to minimize due to that the more the value of this function is lowered, the less exergy is destroyed resulting in a *‘higher quality’* process.

1.2 Objectives

The objectives for this study are separated into two main sections. The first being the theoretical analysis of the thermodynamic process of comminution and the exergy assessment of the laboratory dry ball mill, discussed in the main article in Chapter 2. The second is the application of the studied theory on operational parameters of the laboratory sized ball mill, on a real case scenario of the San Pedro mine plant and a review of the optimization opportunities. Therefore, the objectives can be stated as followed:

a) Thermodynamic theoretical study (Chapter 2)

i) In this section, the first objective is to obtain an adequate relationship to model the comminution energy of the sample material ore followed by its application on the practical minimum comminution work experiment for the laboratory operation size range.

ii) The previous results are fitted into a Hukki-Morrell relationship and then compared to the surface energy or minimal theoretical comminution work and other minimum work models such as inertial calculation for machinery minimum and the Bond relationship.

iii) And thirdly, the application of these comminution relationships and thermodynamic models are applied for the study of the efficiency of a laboratory scale dry ball mill varying for example the boundaries and reviewing inertial calculation results. Results are further reviewed and discussed.

b) Further laboratory review and San Pedro Mine study (Chapter 3)

i) The first objective in this section is to make a further review of the operational parameters encountered in the laboratory experiments and a preliminary approach on developing operational curves based on these results.

ii) This is followed by the application of the developed exergy analysis on the San Pedro mining process throughout the different stages of crushing and fine grinding. This shall be used to detect possible energy savings and identify the major losses.

iii) The third objective will be to compare the results between these real case scenarios with the laboratory and discuss possible factors, such as scaling and the effect between wet and dry ball milling.

2. MAIN ARTICLE

2.1 Introduction

Comminution is the breaking of larger rocks into smaller ones through crushing, grinding, or other processes. In copper mining it is used to crush the ore to a fine powder. In this powder form, flotation tanks can be used to separate the copper concentrate from the gangue (the remainder of the mined material). The comminution process is difficult to optimize because of the irregular (and uncertain) composition and size of the incoming material (Forssberg & Pourghahramani, 2005) and the range of particle loading configurations and failure mechanisms, from brittle fracture to chipping and abrasion (Kapur & Fuerstenau, 1987). In response to this optimization problem, mining and quarry companies tend to use oversized ball mills, jaw crushers, SAG, etc. (Zhao, 2014). On the other hand, since its first reported use in 1870 (Lynch & Rowland, 2005), several improvements have been made to the process by studying the different parameters such as the ball and material load ratio and quantity, ball diameters, performance speeds or the slurry viscosity. Examples of these cases are:

Magdalinovic, Trumic, Trumic, & Andric (2012) on the effect of the rheology of the slurry; Tangsathitkulchai (2003) on crushing balls diameter; Cleary (2001) on the behavior and effects of liner geometry and charge consumption; and Mio, Saito, & Miyazaki (2001) on the effect of ball mill rotational speed.

Much research has been done in the area of energy analysis of systems that undergo material transformations, especially from a manufacturing processes perspective and mostly focused on first law analysis (Bakshi et al., 2011). Although Petela (Petela, 1984) and further on Alvarado (Alvarado, Alguerno, Auracher, & Casali, 1998) both had an interesting exergy analysis on the subject of comminution, their models are focused onto the volume energy of comminution and not much attention is paid to the surface energy, whereas other researchers have focused on this (Ballantyne & Powell, 2014; Musa & Morrison, 2009; Stamboliadis, 2007; Tromans, 2008)**.** The exergy analysis presented in this study considers the chemical exergy of the copper ore, changes to the surface area of the copper ore rocks, the physical exergy of material flows due to temperature changes, the electrical work performed, and the destroyed exergy due to irreversibilities in the process. Alongside a theoretical minimum work we also establish a practical minimum work for comminution based on lab-scale compression tests described below. On the other hand, the minimum work for the ball mill machinery was calculated through an estimated inertial work of the system. All these results are fitted to a previously developed comminution energy relationship and compared with other minimum work estimations. Further on, this information is applied to the exergetic efficiency assessment for a laboratory sized dry ball mill.

2.2 Methodology

All experiments in this study were performed on copper ore taken from a mining plant facility from the central region of Chile with an approximate 2% of copper in mainly chalcopyrite, chalcocite and boronite followed by a 20% of quartz, 19% of plagioclase, 17% of chlorite and 42% of other materials. This resulting in a specific heat capacity, Cp, of 0.302 J/(gK) (calculated through weighted average of the components), a Bond Work Index, K, of 16.6 kWh/ton (provided by the mine plant from where the mineral ore samples were taken), a chemical exergy of 0.837 kJ/g (calculated using Equation (1.9)) and an estimated surface energy of 48.64 mJ/m².

The value of the surface energy was estimated by using a simplified wetting experiment (Biolin Scientific, 2016) done on a material sample. To perform the wetting experiment, a photograph of a droplet of pure water over the material was taken and an image analysis, utilizing the ImageJ Software (Rasband, 2015), was used to measure the contact angle (Krüss GmbH, 2016). This result was utilized with Equation (2.1) obtained from Biolin Scientific (2016) which is a simplified relationship between the contact angle, θ, of the water droplet over the material and the surface energy of water, γ_l ,(Zang, 2013) . The surface energy of the solid material corresponds to γ_s.

$$\gamma_s = \frac{\gamma_l(1 + cos(\theta))^2}{4} \tag{2.1}$$

2.2.1 Experimental Setup

The laboratory procedure consisted of two sets of experiments. The first being the uniaxial compression of the ore, in order to obtain a practical minimum work of comminution expressed as a Hukki-Morrell relationship. The second set of experiments were performed on the dry ball mill in order to determine the exergy efficiency of the experimental process.

For each sample, new material was taken directly from the same stage process at the mining facility (right before ball mill grinding). No samples were reutilized for other experiments as to standardize the incoming material. Samples consist of material ore which is sieved and size selected before the laboratory testing. This is done to standardize the data. The size average and passing 80% product (P80) and feed (F80) case scenarios are considered although, as further discussed, P80 and F80 are used as official results due to the fact it is a better criteria for including the standard deviation of the material size (Bueno, Foggiatto, & Lane, 2015). Average is initially considered as to compare the importance of this dispersion of the grain sizes on energy consumption evaluation.

a) Uniaxial Compression Procedure

The usage of uniaxial compression testing to estimate the energy required for comminution has been used in the past (Haffez, 2012; Mwanga, 2014). Our setup consists of a uniaxial tensile machine equipped with two 5” diameter parallel plates. The rocks are located inside a protective cylinder, large enough to avoid side stresses onto the same and small enough for the sample to fit in and avoid material loss during the compression stage. This is illustrated in the schematic drawing in Figure 2-1.

The samples consist of two size samples 30.84g and 20.86g of particles of diameter 4000μm and 3360μm equivalent to sieves size 5 and 6 on the Tyler scale respectively. Sieving was done according to ASTM D422 standard. This is established considering a mineral size before the ball mill grinding, the size being large enough to adequately perform the experiment, however small enough so the porosity of the material is negligible.

Compression runs at room temperature were performed to calculate the practical work. The parallel plates advance until a compressive load, $\Delta\sigma$, of 100kgf is reached on the sample at the point the rock fragments just starts to break. This indicates that a fair amount of fragments have been rearranged and accommodated so a displacement reference point is established. Relative to this reference point, the machine plates then are displaced a magnitude of $\Delta\varepsilon$ of 1mm; 1.5mm; 2mm; 2.5mm; and 3mm for different samples, respectively, at a fixed rate. A maximum displacement of 3mm is set for two reasons; first due to machine load capacity and second to avoid compaction bands (Das, Nguyen, & Einav, 2013; Guillard, Golshan, Shen, Valdes, & Einav, 2015). According to Issen & Rudnicki (2001), compaction bands are “narrow planar zones of localized purely compressive (without shear) deformation that form perpendicular to the most compressive principal stress”. At about 3mm the compaction bands can be considered almost null and rock breakage is predominant. The displacement rate of the top plate was 0.2mm/min to avoid considerable temperature rise due to friction and to render the process as quasi-static as possible. The load v/s displacement data is then collected to obtain the mechanical work performed in the process. The resulting crushed ores are then collected and sieving is done to determine their particle size distribution. This data was used to calculate parameters for our specific case Hukki-Morrell relationship. This Hukki-Morrell relationship is then employed on our model for practical minimum work.

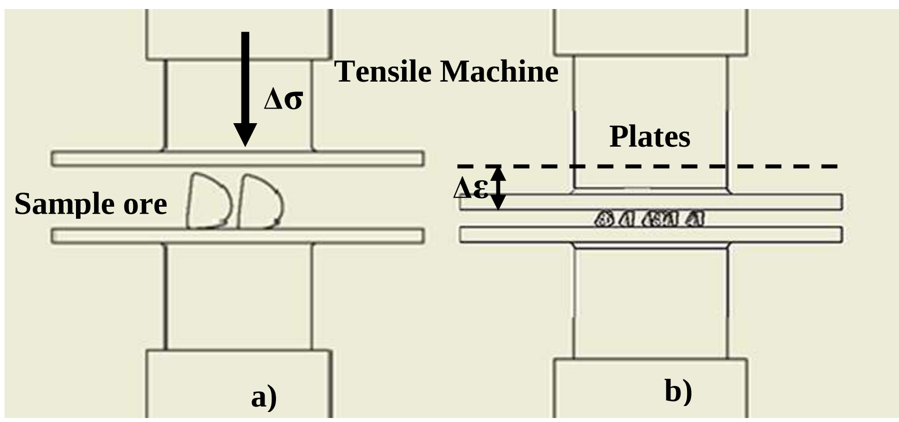

Figure 2-1. Representative schematic of the setup of the compression test.

a) Beginning of test. b) After test.

b) Dry Ball Mill Procedure

These experiments were conducted using a rotatory dry ball mill of diameter 43.18cm and length 60cm. The mill was loaded with an even mixture of 140kg of balls (70kg of 1.5” and 70kg of 2” balls) and 10kg of rock. This results in a weight ratio (balls to rocks) of 14:1 which is representative of industry standard. The mill is rotated at different rpms for different operating times. The maximum rotating speed, limited by the capacity of the motor, corresponds to 64% of the ball mill's critical speed (which is the maximum speed at which the balls are not lifted up or pushed to the shell of the mill and still cascade). A common criteria is to operate at 65-82% of the critical speed (King, 2000). The loaded ore sample was obtained directly from the mine and screened between a US Standard (ASTM E11) ¼ and Tyler 5. These quantities are determined according to the capacity of the ball mill and our ability to measure the outgoing material ore particle size. The electrical work done by the electrical motor that drives the mill, the operation time, and the incoming and outgoing temperatures of the material ore were also recorded.

The ball mill experimental setup is shown in Figure 2-2. The mill is first run empty to determine the amount of work that is consumed as a function of the machine characteristics (mass and moments of inertia). The working balls and the 10 kg of material ore are then loaded inside the mill, processed and the aforementioned parameters are measured. The milled material ore is then removed out of the mill, screened for particle size determination and its temperature measured.

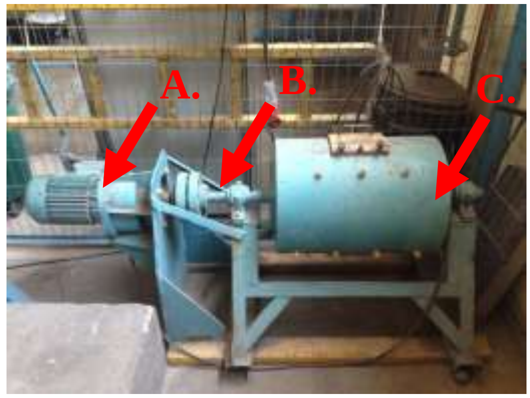

Figure 2-2 Laboratory Dry Ball Mill used in this study, operated in batches.

Where A) Motor B) Reduction gear C) Shell

2.2.2 Exergy Analysis of Ball Mill Grinding

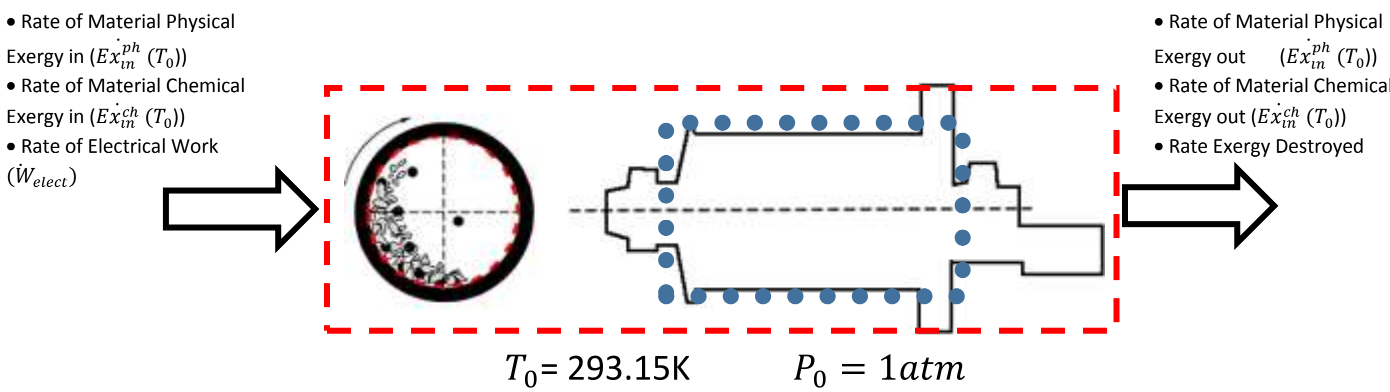

Figure 2-3 Dry Ball Mill mass and energy rate diagram and control volume selected

To be able to carry out exergy calculations it is necessary to define the reference state and the physical boundaries of the system, as shown in Figure 2-3. The first boundary considered is outside the ball mill and, therefore, the material enters the system at ambient temperature, T_o . Electrical work rate applied, $\dot{W}_{elect}$, also enters the system. The exiting material has cooled down to ambient temperature. For exergy balance we also label the destroyed exergy rate, $\dot{E}x_{des}$, as leaving the system. We define this first boundary as BOUNDARY 1 (outer box in Figure 2-3). Another boundary is defined as BOUNDARY 2 (inner box in Figure 2-3) which considers an optimization case in which the heat of material after comminution is saved so the exergy destroyed is reduced as the heat energy in the outgoing material could be used in another process.

The next step is to obtain the minimal work for comminution from the exergy rate balance equation. For this, it is important that there be no heat losses so it can be considered as a perfectly adiabatic system, therefore we establish a condition of zero temperature increase within the system. Moreover, within this definition of a *'perfect process'* we consider establishing the case that $\dot{E}x_{des} = 0$, which means that the process is ideal and reversible, and that the comminution work considers only the chemical exergy and surface exergy work terms.

$$\dot{E}x_{in_{ch}}(Ti) + \dot{W}_{min} = \dot{E}x_{out_{ch}}(Ti) \tag{2.2}$$

This leads to Equation (2.2) in which $\dot{W}_{min}$ represents the minimal work rate for performing the comminution process of the material ore. The work relationships developed by Bond (Bond, 1952), Rittinger (Rittinger, 1867) or Kicks (Kick, 1885) express the comminution work of optimized ball mills. In this study we will consider two types of minimal work: theoretical minimum and practical minimum. A theoretical minimum considers for example the surface energy difference and does not account for other major losses in comminution such as entropy, heat rising (although minimal or negligible), displacement, etc. On the other hand, practical minimum shall consider practical non-idealized real cases in which comminution can occur. Following this latter scenario, the minimal practical work is made equal to the work obtained from our uniaxial compression test. We consider that there is minimal heat generation due to the slow compression rate. This method resulted in determining the parameters of the Hukki-Morrell relationship for our material by using the force results per displacement, registering the initial and final ore size distribution. Thus, obtaining the corresponding energy and solving the equation maintaining the fixed material constant fixed to obtain the value of the Hukki exponent.

Using the Hukki-Morrell relationship obtained as the practical minimum work, we can then calculate the following efficiency measures: Equation (2.3) for boundary 1, and Equation (2.4) for boundary 2. In the latter equations, since the efficiency is evaluated in a defined interval of time, then the instant rate is turned into a discrete and fixed change of property. Therefore, in these equations, η_P is the efficiency, $W_{p,com}$ the comminution work, $Ex_{elect,W}$ the exergetic work provided by the electric motor, $Ex_{ph,in}$ and $Ex_{ph,out}$ the incoming and outgoing physical exergy of the material respectivly.

$$\eta = \frac{W_{p,com}}{Ex_{elect,W}} \tag{2.3}$$

$$\eta = \frac{W_{p,com} + (Ex_{ph,out} - Ex_{ph,in})}{Ex_{elect,W}} \tag{2.4}$$

However, utilizing the Hukki-Morrell relationship is equivalent to consider a general case for comminution, such as to compare different methods to perform the work. To the specific case of the ball mill machinery efficiency, an inertial work calculation of the drum and ball charge can be done and considered as the minimum work for the ball mill machinery due to that it is a better benchmark to fairly assess the energy of the specific machinery process. This is what we will define as the practical minimum work for the machinery. This minimum work can be generalized by the minimum inertia of the system to operate, as seen in Equation (2.5). Where I_{Mill} is the moment of inertia of the ball mill drum, ω_{Mill} the angular velocity of the ball mill drum, T_{Balls} torque due to the position of the balls relative to the center of rotation of the mill (Mishra & Thornton, 2002) and τ time. Figure 2-4 illustrates the free body diagram which leads to Equation (2.5).

$$E = \frac{1}{2} I_{Mill} {\omega_{Mill}}^2 + \mathrm{T}_{Balls} \cdot \omega_{Mill} \cdot \tau \qquad (2.5)$$

The torque to energy calculation, $\mathrm{T}_{Balls} \cdot \omega_{mill} \cdot \tau$, is used to characterize the rotation of the mill in a given time and speed standardized to one second. Therefore, rpm can characterize the torque applied to the mill by converting it to rad/s and then evaluating how much the mill rotated during that second. Moreover, the torque calculation is given by the weight of the ball and material load multiplied by the distance given by the angular position of the center of mass of the rotating balls inside the ball mill. This angular position corresponds to the angle α which is given by the horizontal line and the point in which the highest ball is lifted up due to the forces governing its movement.

On the other hand, $\emptyset$ is the angle the highest layer of the load forms with the radius of the highest/lowest contact point with the shell of the ball mill (Figure 2-4). For simplicity, we suppose that the load behaves as a uniform mass in which the upper layer of balls behaves linearly and depends on the percentage of fill of the ball mill, as seen in Figure 2-4. Equation (2.6) obtains the angle α in which R is the inner radius of the mill, r the radius of the balls in the mill, g gravity and ω the angular velocity (Karunatilake et al., 2000).

$$\alpha = Arcsin\left(\frac{(R-r)\omega^2}{g}\right) \tag{2.6}$$

Most early researchers considered the uniform mass assumption (Miller, Young, Kellar, & Free, 2005) but today a dynamic model is used to model the ball position utilizing discrete element methods, as for example studies made by Dong & Moys (2003). There are various other ways to calculate this position *A*. Bai, He, Fu, & Han (2014) made a similar approach to Mill et al. (2000) which in practice gave the same number. On the other hand, Davis for example, developed a positioned circle over the ball mill center of rotation in which its position and radius is given principally by the angular velocity and the intersection of this imaginary circle with the ball mill inner perimeter gives the position A (Davis, 1919; Miller et al., 2005). This idea was followed and further developed by Hogg & Fuerstenau (1972) and Rose & Sullivan (1958) which later turned to base the discrete element method to simulate ball mill behavior.

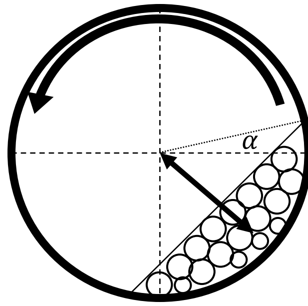

Figure 2-4 Free body diagram illustration of the minimum inertial moment energy

Therefore, the energy consumption estimate given by inertial calculations as a function of rpm can be given by the general Equation (2.7). Here, M_{total} refers to the total mass of the balls and the processing material, *CM* the center of mass of the load, $\emptyset$ the angle the highest layer of the load forms with the radius of the highest/lowest contact point with the shell of the ball mill (Figure 2-4), *R* the inner radius of the drum, *r* the radius of the balls, *rpm* the angular velocity of operation and *g* gravity.

$$E_{inertial} = \left(\frac{1}{2}I_{Mill}\omega_{Mill}{}^2\right) + \left(M_{total} \cdot g \cdot CM \cdot sin\left(\left(\frac{\pi}{2} - \emptyset\right) + Arcsin\left(\frac{(R-r)(2 \cdot \pi \cdot rpm)^2}{g \cdot 3600}\right)\right) \cdot \omega_{mill} \cdot \tau\right) \quad (2.7)$$

Another important situation is to consider the scenario in which the material exergy is much higher than the process's exergy, as it can be sometimes misleading when developing exergy assessments. As this later practice shows, when the material's exergy (chemical and physical) is higher carrying alongside the temperature rise and other factors as products, the efficiency rises to unrealistic optimist values. This effect is in other words called '*Transit Exergy'*. Another example of this is done in Bakshi et al., (2011) with an electrical furnace and gives a clear example on the subject. The value of this study's transit exergy efficiency is shown further on using Equation (2.8) obtained from Chapter 6 in Bakshi et al., (2011) although again, since we are evaluating in a defined interval of time, for this assessment we shall turn the instant rate into a discrete and fixed change of property.

$$\eta \quad = \frac{Ex_{product}}{Ex_{in}} \tag{2.8}$$

Where $Ex_{product}$ refers to the exergy rate of the wanted product leaving the boundary and Ex_{in} the incoming exergy into the system boundary.

2.3 Results and Analysis

2.3.1 Uniaxial Compression Tests

The uniaxial compression tests resulted in a curve that represents the real comminution energy in Joules consumed by the material during the compression process. The slope variation of the force v/s displacement curve in Figure 2-5 and Figure 2-6 is probably caused by the capsizing of interstitial porosities and the increase in the surface area of the rock (Yavuz, Altindag, Sarac, Ugur, & Sengun, 2006). Figure 2-5 shows an example of estimating this curve using a fitted function.

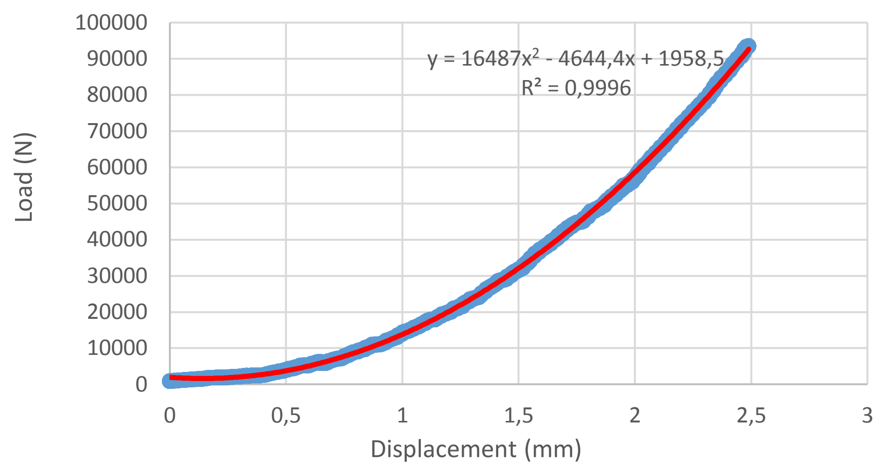

Figure 2-5 Example of an obtained fitted function as to calculate the work done by the uniaxial compression machine

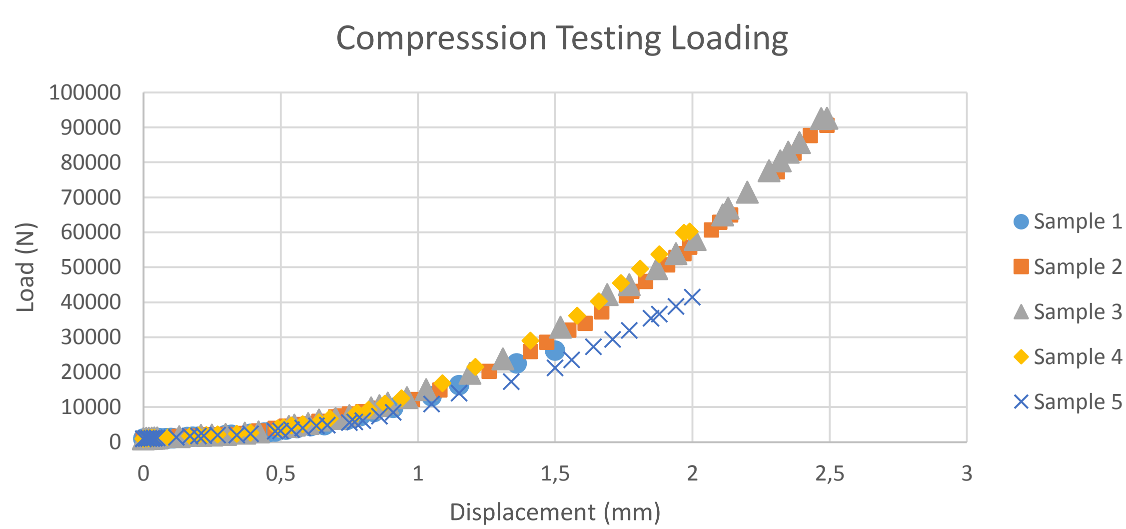

Figure 2-6 Load v/s Displacement for several uniaxial compression results. Graph shows a subset of the experimental results

Table 2-1 shows the results obtained from the uniaxial experiment considering average and passing 80% of incoming and outgoing particle size. The third row represents the minimum practical comminution work obtained integrating the curve from Figure 2-6 through estimates such as presented in Figure 2-5. The fourth row shows the theoretical minimum comminution work according to the Bond relationship as to compare the test with a known relationship.

Values of the Hukki's exponential term *f(x)* were obtained at discrete ranges and are presented in the uniaxial compression results in Table 2-1. These exponent values were plotted in Figure 2-7 as to observe any relationship between them. The exponents were calculated using the solver add-in of Microsoft Excel® adjusting the best exponent for each range minimizing the squared difference of the resulting value to what was empirically obtained. An important note is that the various optimum solutions were obtained, the selection of the solution which best fits our study is given by the one which fits for a larger range of results. This was done graphically but it is recommended that future research considers a larger size range as to reduce the error when assessing projected ranges. The latter figure, a linear relationship such as what was proposed by Morrell was found. This linearity will be used as to project the material's behavior for the rest of the operation range.

This low approximation capability is due to that, although the exponents seem to have a linear behavior, there is still a good deal of scatter amongst them. This scatter persists with the addition of more data points. Therefore, even though Morrell was correct on noticing the linearity, this relationship must be considered with caution when assessing due to the error margin. The exponent function is shown in Table 2-6.

Table 2-1 Hukki curve f(x) parameter values for a practical minumum work model from uniaxial compression testing results. Incoming grain size is 3.675mm ±0.325mm and Passing 80% of feed of 3.9mm.

Displacement (mm)	2.72	2.49	2.49	2	1.99	1.5	1
Sample Weight (kg)	20.69	30.665	30.665	20.705	30.81	30.665	30.675
Minimum Comminution Work (kWh/ton)	1.062	0.682	0.654	0.367	0.353	0.127	0.040
Bond (kWh/ton)	0.982	0.488	0.422	0.370	0.360	0.234	0.194
Average Outgoing Grain Size (µm)	1629.918	2230.182	2331.713	2520.632	2605.369	2866.763	3411.263
Passing 80% Product (P80, µm)	2079.153	2784.2	2904.726	3005.926	3024.925	3294.127	3388.68
Standard Deviation Outcome (µm)	992.12	1068.69	1075.68	1018.47	992.42	955.78	567.57
Hukki Exponent (f(x))	-0.372	-0.414	-0.417	-0.487	-0.490	-0.486	-0.741
Hukki Exponent P80 (f(x))	-0.269	-0.284	-0.285	-0.306	-0.307	-0.326	-0.331

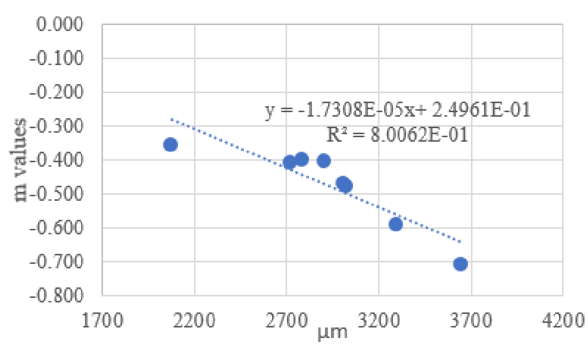

Figure 2-7 Uniaxial compression testing exponential values for the Hukki-Morrell relationship using passing 80% size criteria. All samples from the same initial size, showing the validness of Morrell’s observation.

Figure 2-8 shows the Hukki-Morrell relationship integrated from infinity to the specific grain size form using the discrete values for *f(x)* from Table 2-1 along with the empirical data points. Note that work done by the uniaxial compression machine provides the energy difference between the incoming and outgoing material ore size. On the other hand, to obtain a curve suited for a larger size range, the direct measurement of the laboratory experiment cannot be used. This is due to the boundary conditions of the integral which must be modified to begin at infinity and end at the wanted grain size. This is to avoid any convergence to a number when plotting the whole size range, as seen in Figure 2-8. In this case, the laboratory experiment would be equivalent to the integration from 3900μm to the end product size. Therefore the uniaxial compression testing is useful to obtain the parameters but not for plotting directly the whole size range of minimum energy required for comminution. As seen in the latter figure, these curves provide a lower comminution work values in kWh/ton than when using Bond relationship.

As seen in Figure 2-8, there is a considerable difference in energy when using an average or a passing 80%. The reason why most researchers use the passing 80% is to assure in a practical and simplistic manner, the evaluation of the material considering the dispersion of sizes (Bueno et al., 2015). Ideally, the passing 80% should be close to the average, but in a worst case scenario then the dispersion must be taken to account. This passing 80% is a practical way to overcome this difficulty but a relationship which directly utilizes the standard deviation or other dispersion parameters would result in a more accurate assessment of comminution energy. For this study, we shall employ the practical approach for considering dispersion and use the passing 80%.

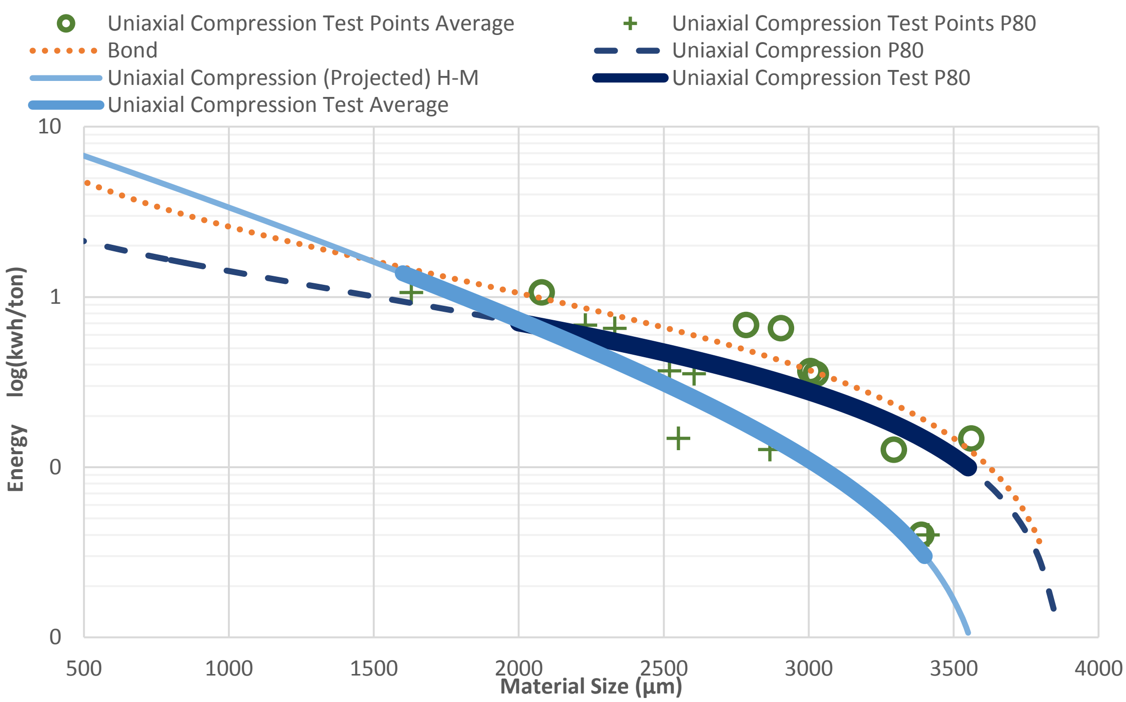

Figure 2-8 Integrated Hukki-Morrell curve obtained from uniaxial compression of the material testing and Bond curve from the initial sized ore using average and P80 ore size criteria.

A key observation to note is that, from the comminution processes studied by uniaxial compression, this estimates more realistically the physics involved in the process, as it represents the lowest work applied to obtain the same particle size. Therefore, we shall use the information from the Hukki-Morrell fitted relationship to establish the minimal work of comminution when, considering any further efficiency analysis of the dry ball mill procedure.

Although the relationship offers a good estimate on the comminution energy for the studied size range, it does not have a good relationship with much smaller sizes. The reason is due to the inefficiency of the machinery to perform further comminution after a certain size. This latter is frequently seen in practice in several mining plants and furthermore relates to the importance in machinery selection for different ore reduction size (Metso, 2010). In this case the Bond relationship is designed for fine grinding in sizes such as 100-1000μm in which ball milling is more efficient than compression, therefore resulting in a better relationship in said ranges. In our case, the uniaxial compression represents well the range of operation therefore this shall not become a problem during the course of this study.

It is important to also emphasize that although we shall use this definition, this is not the theoretical minimum comminution work but more of a practical minimum comminution work. This is due to the fact the comminution is highly irreversible. In order to model a reversible comminution process, surface energy data obtained for our sample material ore from literature (Douillard, Salles, Henry, Malandrini, & Clauss, 2007; Marshall, Barnhart, Shappee, & Most, 2015; Mattew, 2010) and by wetting experiments; resulted in 48.64 mJ/m^2. This result represents the true minimum work for comminution per unit area generated and is the parameter that ought to be used to calculate the minimum work term in Equation (2.2). However, this method implies minimum work values that are 10^{-13} times lower than the practical minimum comminution energy.

On the other hand, in Figure 2-9, the total energy results for different displacements are shown for the same uniaxial income size (3900μm) along with an estimate relationship utilizing surface energy, elastic compression energy and friction energy. It is interesting to note there seems to be a correlation based on these latter that fits well to the laboratory results therefore giving emphasis that these should be the parameters that defines the increment proportion in comminution energy and therefore is highly related to the previous comminution energy relationships.

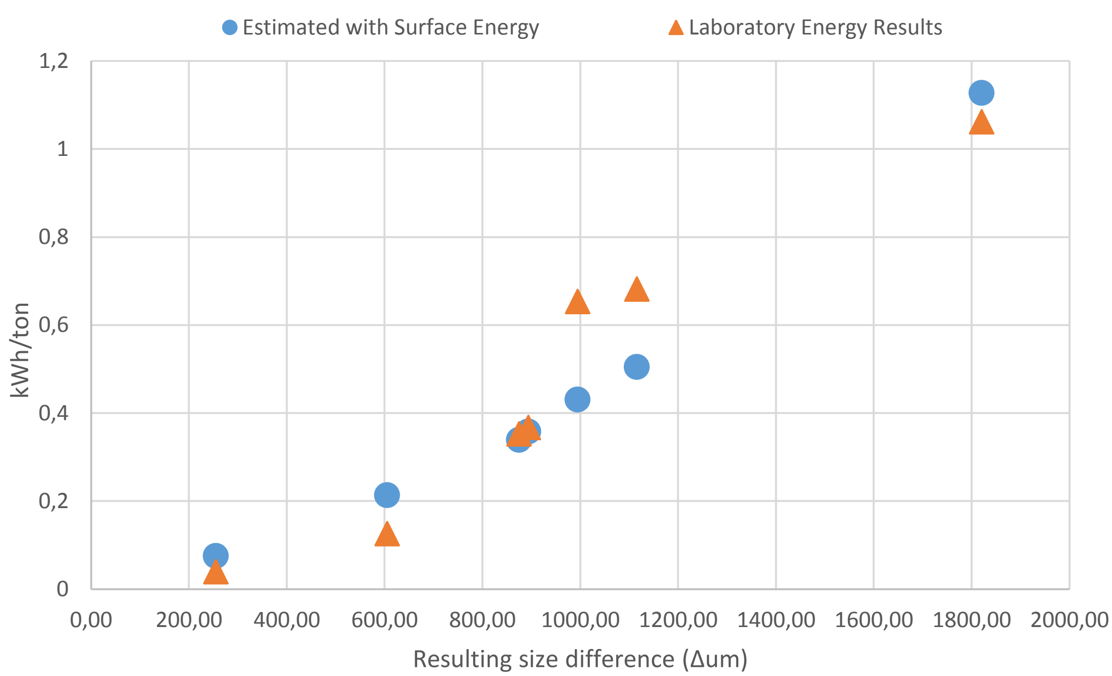

Figure 2-9 Compression test energy consumption (same initial size, 3900 um)

2.3.2 Dry ball mill results

c) HUKKI-MORRELL RELATIONSHIP

Dry ball mill tests results are shown in Table A-4 (annex). Considering now the Hukki-Morrell curve (as the practical minimum work for the material ore) has been constructed from the uniaxial compression comminution process, the exergy efficiency values of the dry ball mill comminution process can be obtained too. However as seen in the comminution work curves in Figure 2-11, a Hukki-Morrell curve was also obtained for the dry ball mill process as to compare against the uniaxial compression and denote the importance on the machinery used to obtain Hukki-Morrell relationships. This was done from the electric energy consumption of the motor for different resulting grain sizes, as seen in the ball mill experimental data in Table 2-5.

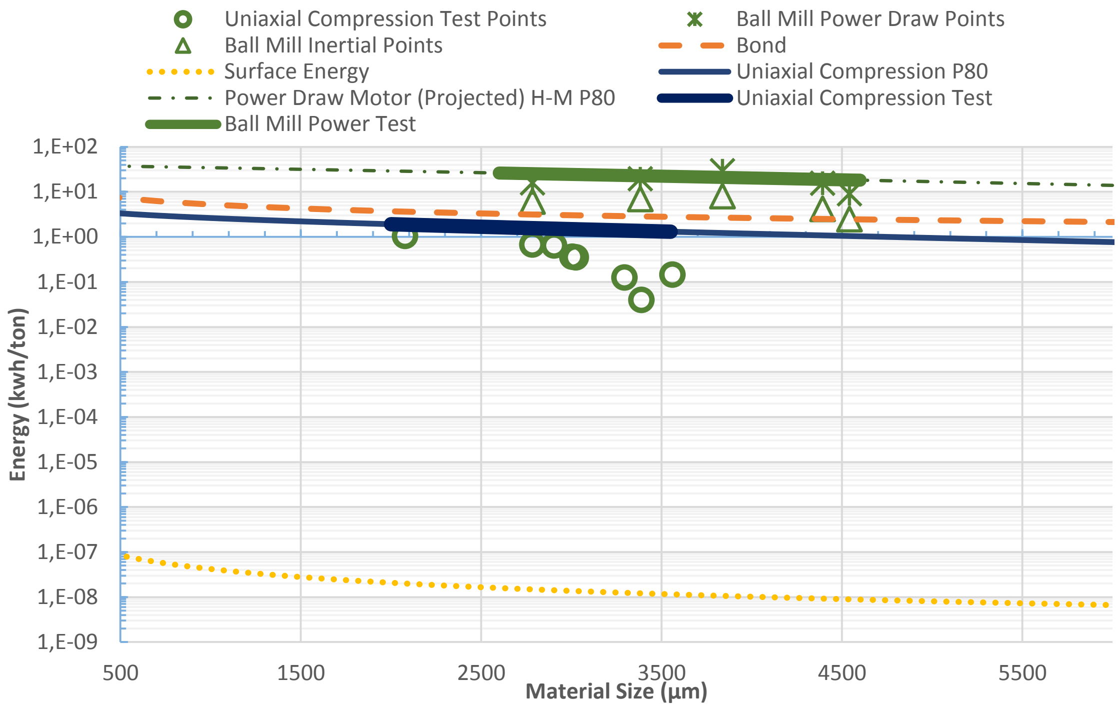

Figure 2-10 General view graph of the integrated Hukki-Morrell curves obtained from inertial calculation, the practical minimum work from compression testing, ball mill testing and Bond curve from an infinity sized ore.

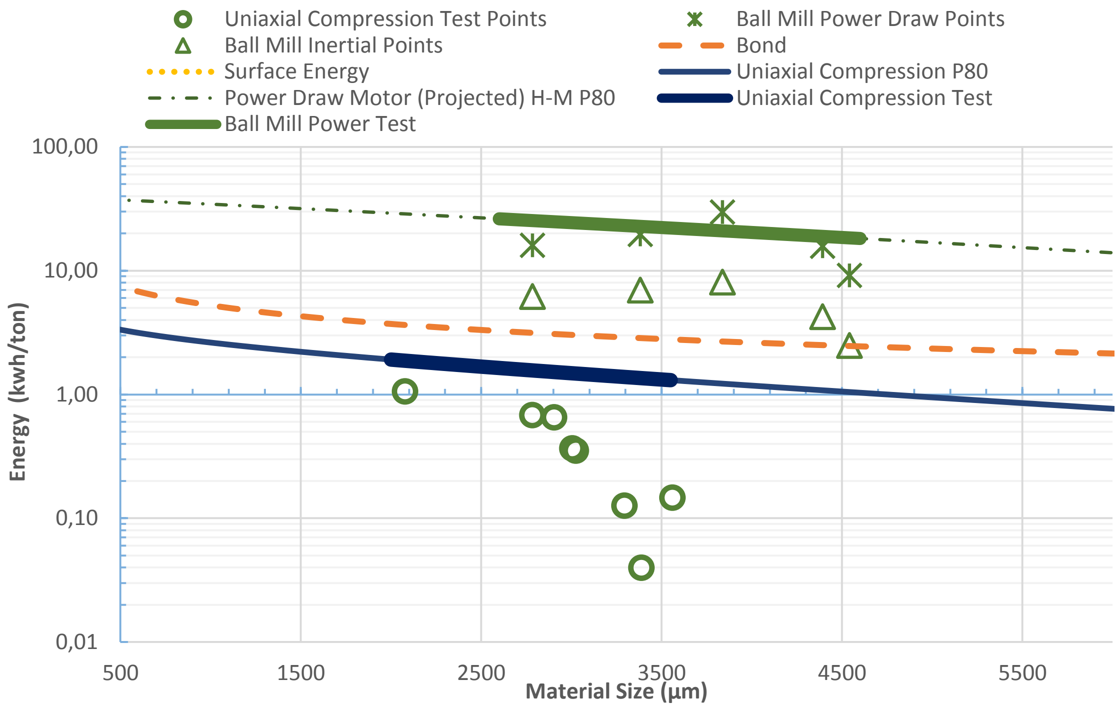

Figure 2-11 More detailed graph of the integrated Hukki-Morrell curves obtained from inertial calculation, the practical minimum work from compression testing, ball mill testing and Bond curve from an infinity sized ore.

2.3.3 Baseload Electric Power Draw of Ball Mill

In order to investigate the energy consumed by the dry ball mill, a measurement of the electric power drawn with and without load was taken from the laboratory ball mill and illustrated in Figure 2-12. As shown by Figure 2-12 a first opportunity to optimize the ball mill is to reduce the inertial resistance of the operation and to ensure that the motor capacity is appropriate to the work required. It was estimated that the average efficiency when rotating the cylinder, using inertial calculations, is 1.77% without load and 22.03% with the 150kg load. As for the material ore, as seen in Figure 2-12, it does not affect the consumption value much due to the similar load ratio. This suggests that the amount of balls or material ore does not majorly affect the overall efficiency and that they are viable optimization parameters as some researchers have studied. For example Cleary (2001) studied on the effect of fill changes, liner shape, liner pattern and ball charge; and Sahoo (2014) studied particle sizing, density of materials and number of balls.

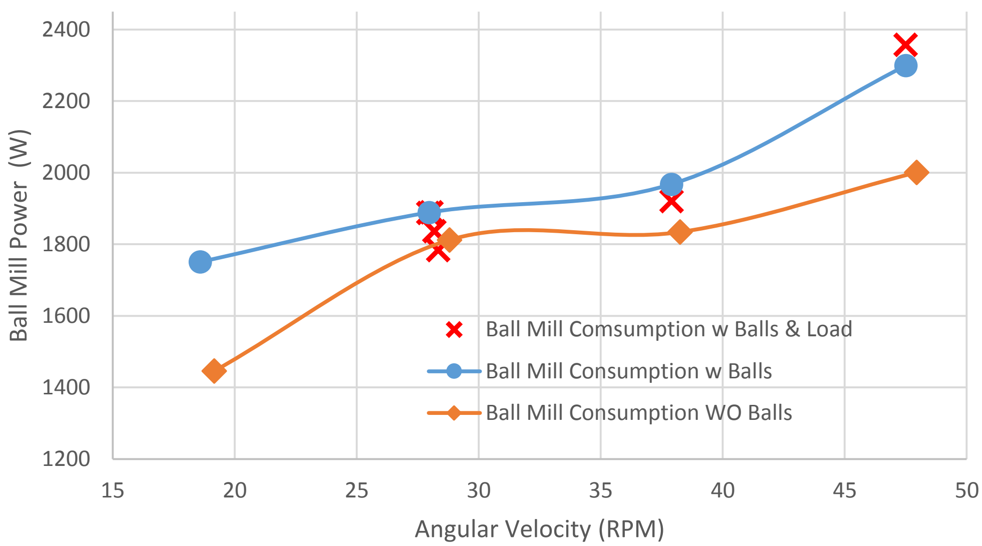

Figure 2-12 Power consumed by system without material load (only shell and balls), which is similar to material load due to the similarity of ratios (14:1 and 15:1)

It is interesting to compare these latter results with an industrial wet ball mill. Reviewing a wet ball mill from a mining facility associated with this research team, the power consumed by each process seems to show a scaling shown in Table 2-2. The wet versus dry ball mill operation difference is considered by using a fraction of the electric current consumed in the wet ball mill which is given by the ratio of the solid/liquid charge. Moreover, the energy difference between an unloaded and loaded operations grows with the radius of the ball mill as seen in the last rows of the first column of Table 2-2. Although these results deviate from the main discussion, this scaling factor would be interesting to further review in future research.

Table 2-2 Operational parameters between the laboratory sized ball mill and a real wet ball mill from an associated mining facility. Both operations at 25 rpm

<table>
<tr><th>Mill</th><th>Diameter (m)</th><th>Length (m)</th><th>Throughput (kg/hr)</th><th>Power w/o balls (W)</th><th>Power w balls (W)</th><th>Inertial energy drum (J)</th><th>Inertial energy torque balls (J)</th><th>Volume (m^3)</th></tr>
<tr><td>Minera San Pedro wet ball mill (MSP)</td><td>1.80</td><td>3.00</td><td>4166.67</td><td>21061.74</td><td>42781.65</td><td>27953.87</td><td>28179.18</td><td>7.63</td></tr>
<tr><td>Laboratory dry ball mill (LAB)</td><td>0.43</td><td>0.60</td><td>125.08</td><td>1628.99</td><td>1819.87</td><td>16.16</td><td>160.46</td><td>0.09</td></tr>
<tr><td></td><td></td><td></td><td></td><td></td><td></td><td></td><td></td><td></td></tr>
<tr><th></th><th>ΔPower (W)</th><th>ΔEnergy Inertial (J)</th><th>Δ Power/ Throughput (Whr/kg)</th><th>Δ Inertial Energy/ Throughput (J hr/kg)</th><th>Δ Power MPS/ΔPower LAB</th><th>Δ Inertial Energy MSP/Δ Inertial Energy LAB</th><th>MSPvolume/ LABvolume</th><th>Δ Inertial Energy TP MSP/Δ Inertial Energy TP LAB</th></tr>
<tr><td>Minera San Pedro wet ball mill (MSP)</td><td>21719.9</td><td>28179.18</td><td>5.21</td><td>6.76</td><td rowspan="2">113.78</td><td rowspan="2">3.42</td><td rowspan="2">195,28</td><td rowspan="2">5.86</td></tr>
<tr><td>Laboratory dry ball mill (LAB)</td><td>190.9</td><td>144.3</td><td>1.53</td><td>1.15</td></tr>
</table>

On the other hand, when calculating the theoretical inertial energy consumption work the ball mill should have, the results show that the main energy of the system is used on the torque of the steel balls and processing material load. The results of the corresponding lift angle, total, specific energies of the torque and inertial rotation of the drum of the ball mill are shown in Table 2-3 and the percentage of participation of each work requirement in Figure 2-13. The latter identify the torque component as the most energetically dominant requirement in the ball mill process in which optimization on the process would be more influential.

Table 2-3 Summary of inertial and torque values for the different samples

Sample	RPM	Lift Angle (rad)	Motor Average (W)	Theoretical Total Power (W)	Theoretical Drum Power (W)	Theoretical Ball Power (W)	Inertial Efficiency
1	47.50	0.52	2009,20	714.54	53.75	660.79	0,36
2	27.93	0.1806	1887,66	309.75	21.75	288.01	0,16
3	28.19	0.1806	1836,32	301.33	21.15	280.17	0,16
4	28.07	0.1806	1888,97	309.97	21.76	288.21	0,16
5	28.35	0.1806	1783,67	292.69	20.55	272.14	0,16
6	47.50	0.52	838.44	63.07	775.38	775.38	0,36
7	37.90	0.3223	512.58	38.21	474.38	474.38	0,27

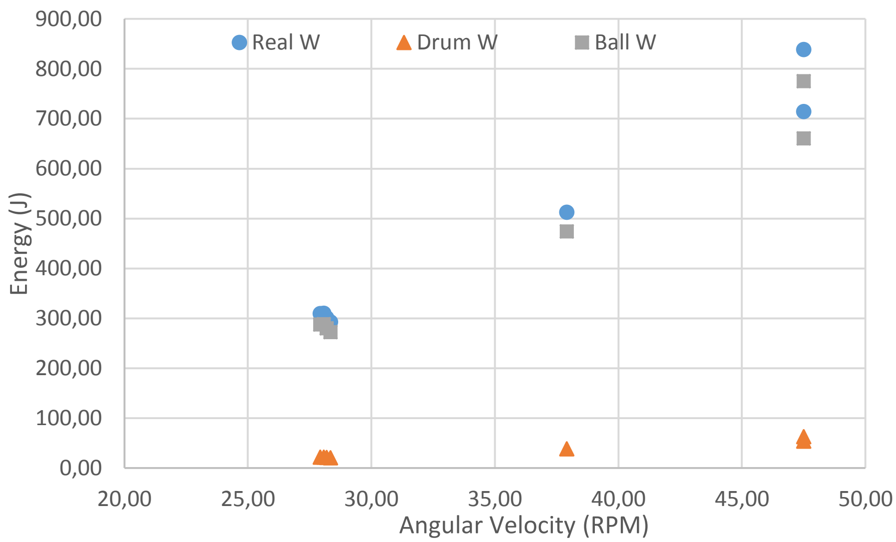

Figure 2-13 Theoretical mill energy consumption due to inertial work to rotate the drum and the torque required due to ball weight and displacement

Moreover, as seen in Figure 2-11, the Hukki-Morrell relationship obtained from the power draw of the ball mill is not as efficient (regarding the energy consumption of the process) as the theoretical Bond comminution work but at the same time, Bond's comminution work isn't as efficient as the Hukki-Morrell relationship obtained by the uniaxial compression testing. It is important to emphasis that the solution given by Figure 2-11 is a local optimum which fitted well along the projected size range. In fact, reviewing the other local optimums, the uniaxial compression testing does not predict well fine grinding as would an optimized ball mill such as proposed for Bond Work Index studies (Bond, 1961). Therefore, it is of importance to review the machine used for establishing the Hukki-Morrell parameters. Since the apparent point of which uniaxial compression becomes less efficient than ball milling is lower than our operation range, then this is not a problem for this study. Therefore, for higher ore size assessments, uniaxial compression testing is a good measurement for practical minimum energy.

2.3.4 Exergy Efficiency

The exergy analysis results obtained are presented in Table 2-4, Table 2-5, Table 2-6, and Table A-1(annex). The data in Table 2-6 consists of the summary of all the reviewed efficiencies including the linear exponent proposed by Morrell. The first and foremost observation is that utilizing surface energy results on a impractical analysis due to the results were of an efficiency of a $4.30 \cdot 10^{-13}$ reassuring that the main losses are due to the irreversibility of the process.

The transit exergy results are shown in Table 2-4. As stated before, this model for energy efficiency leads to error. This error is given by considering the materials exergy as the objective and not the process itself. As seen in Table 2-4 and Table 2-6, if transit exergy were to be considered, then the ball mill process (and most comminution machinery) would be considered efficient, contrary to what really happens when considering non-transit exergies.

Table 2-4 Transit exergy assessment results. Chemical exergy 0.837kJ/g

	Sample 1	Sample 2	Sample 3	Sample 4	Sample 5	Sample 6
Exergy In (kWh/ton)	24.65	24.41	24.33	24.45	24.28	24.37
Exergy Out (kWh/ton)	24.67	24.42	24.34	24.48	24.30	24.40
Comminution Work H-M (kWh/ton)	0.43	0.29	0.33	0.63	0.85	0.49
Mechanical Work In (kWh/ton)	14.33	9.20	15.76	29.91	19.65	16.05
Efficiency (%)	64.70	72.73	60.89	45.92	56.79	60.94

It was also noted by using a first law assessment and the minimum practical work for comminution, that not all the electrical energy going into the system is transferred into the heat rise of the outgoing material nor into the comminution work. Without considering the irreversibility of the process, the main source of losses is heat lost to the environment through the gear box and the shell of the mill. Table 2-5 and Table A-1 show that the exergy efficiency is of the order of 2.97% for the first boundary (outer dashes in Figure 2-3 where outgoing temperature equals incoming and ambient temperature) and a 3.08% for the second (inner dots in Figure 2-3 where the outgoing temperature, average 15.5ºC, is higher than the incoming and ambient, average 15.4ºC). On the other hand, considering that the minimum work for a dry ball mill *per se* as the comminution work is not entirely valid. To use the inertial energy required to spin the mill as the minimum work is the most valid method to review the machinery efficiency. Considering this inertial energy the efficiency increases to a 21.32%. This inertial energy for the ball mill was calculated using Equation (2.5) and shown in Table 2-3. This efficiency value differs from the inertial efficiency of the machinery mentioned previously due to that this efficiency is not only evaluated with respect of the operation rotational speed but correlates that same rotational speed with the resulting grain size as well with considering the repetition of certain sample speeds (given within the same six samples). Moreover, when the mill is unloaded the work to spin the drum is highly inefficient as seen in Figure 2-12. It was calculated that in the unloaded operation, the machine has an efficiency of an average of 1.77% without load and 22.03% with the 150kg load. This implies that the main loss is not in the heat lost in the shell rather more it is the heat lost through the transmission system that spin the mill and that the recapture of the heat rise of the material as to increase efficiency would not be of a major impact.

Table 2-5 Dry ball mill testing results. Chemical exergy 0.837kJ/g

Load Factor	Grain Size F80 μm	Grain Size P80 μm	RPM	Tamb °C	Tin °C	Tout °C	Time min	Total Rev	Motor Average W	Dry Ball Mill Comminution Work kWh/ton	Minimal Comminution Work Compression kWh/ton	Minimal Comminution Work Theoretical kWh/ton	Δ Physical Exergy for Boundary 2 kWh/ton	Bond kWh/ton	Exergy efficiency Boundary 1	Exergy efficiency Boundary 2 %
12.80	3900	2643.10	27.9	17.9	16.1	17.7	5	139.6	1491.25	14.33	0.43	1.95E-15	0.0218	0.571	3.03	3.18
14.07	5840	4542.47	28.2	15.3	14.2	14.9	3	84.6	1450.69	9.20	0.29	4.50E-15	0.0095	0.291	3.18	3.28
14.06	5840	4342.91	28.1	14.4	14	14.6	5	140.4	1492.29	15.76	0.33	7.78E-15	0.0083	0.332	2.10	2.16
14.13	5840	3381.94	28.3	15.8	13.9	16.3	10	283.5	1409.10	29.91	0.63	3.54E-15	0.0327	0.682	2.12	2.23
14.05	5840	2785.23	47.5	14	12.8	14.2	5	237.5	1862.50	19.65	0.85	8.08E-15	0.0190	0.973	4.32	4.41
14.08	5840	3838.05	37.9	15	13.5	15.4	5	189.5	1517.25	16.05	0.49	4.72E-15	0.0256	0.507	3.04	3.20

Table 2-6 Summary of the efficiencies reviewed in the study.

Index Criteria	Bond	Ball Mill Hukki-Morrell Boundary 1	Inertia Hukki-Morrell Boundary 1	Compression Hukki-Morrell Uniaxial Boundary 1	Compression Hukki-Morrell Uniaxial Boundary 2	Surface Energy	Transit Exergy
Exponential Linearity	0.5	-4.8612E-05x + 1.1520E-01	N/A	-1.7308E-05x-2.4961E-01	-1.7308E-05x-2.4961E-01	N/A	-1.7308E-05x-2.4961E-01
Average Comminution Work kWh/ton	0.56	17.48	3.77	0.50	0.50	7.62E-14	0.50
Average Efficiency %	3.27	100	21.32	2.97	3.08	4.30E-13	60.33

2.4 Main Article Conclusions

This study on copper ore comminution has led to several findings:

a) A uniaxial compression procedure to achieve comminution can provide a better model of the real physical phenomena involved in the process.

b) Because its variable exponent *f(x)* can be fitted in several particle size ranges according to the experimental data, a Hukki relationship along with Morrell's exponential linear estimation can provide a more accurate estimation for comminution energy density values. At the same time, since a uniaxial compression procedure has shown to require the least amount of work density to achieve material ore comminution in the required ore size range, its usage along with a Hukki-Morrell relationship modeling has proven to be effective. Therefore it can be considered to be a closer and more practical method of modeling the real comminution process energy for the wanted particle size range.

c) Although the uniaxial compression method has proven to be effective, the importance in obtaining precise exponent values to obtain the linearity proposed by Morrell has been proven necessary for a correct assessment. Therefore, a sufficient amount of data points throughout the range is necessary to make correct projections of the comminution work.

d) It is important to keep in mind that although Hukki-Morrell is a better representation for comminution work for material ores, it is highly dependent on the process (such as jaw crushing, cone crushing, ball milling, rod milling, etc.) from which it was obtained, therefore its effectiveness varies between experiments. This should be considered for future studies.

e) Although surface energy analysis is accurate on determining the minimum energy required for comminution, it results to be unpractical for an industry assessment due to the extremely low energy value and the inevitable irreversibility (given by the new surface area generated) in the process and does not aid much in evaluating practical grinding processes.

f) As discussed in the exergy analysis, comminution energy in the dry ball mill is marginal compared to the total energy of the process and most of the energy is spent on keeping the system's mass in rotation.

g) Energy saved by heat capturing in dry ball milling represents about 0.11% of an operation efficiency increase. This low improvement is due to the low temperature difference in income and outcome heat of the material and they are highly close to the reference point, the ambient temperature. Therefore this factor of optimization would not be of major impact.

h) Adequate electric motor, transmission selection and machinery scaling are a fundamental factors for optimizing energy. These factors should be studied for each case for an adequate operation and desired optimal operation standards as well as be considered for future research and development.

3. FURTHER LABORATORY REVIEW AND MINING PLANT ASSESTMENT

3.1 Introduction

In the San Pedro mining plant, crushing and fine grinding uses approximately 90% of the total energy consumption for operation, being the wet ball mill fine grinding the main energy consumer with a 72% usage of the total energy of the plant (Private conversations with Minera San Pedro, 2015).

The comminution process of the plant courses as follows: In the first phase, crushing, the main objective is to reduce the mineral size that arrives directly on trucks from the mine digging site down to as small as the income of the ball mill can process (approximately 3650um, all values are on average). In this plant, the crushing phase is done in three stages: primary jaw crushing (to 74.93 mm), secondary (to 16.64mm) and tertiary cone crushing (3.65mm) with a production rate of 60 ton/hr. The next phase, wet ball milling, will then fine grind the mineral down to a size in which the copper sulfate particles can be retrieved in the flotation cells (approximately 200um) of the following stage. The ball mill phase is a single stage process which has a production rate of 12.5 ton/hr of the copper ore.

The following chapter study reviews the data obtained from Chapter 2 and applies the exergetic rate of the laboratory sized ball mill to review parameters such as work applied, income and outcome temperatures, operation time, mass load and ball mill speed. From this information, estimates for operational curves have been proposed. Moreover, we shall also review the crushing and grinding process for this copper mine plant utilizing the concepts described previously in Chapter 1 and will furthermore use the parameters obtained and analysis developed in Chapter 2 to compare the results from the latter chapter with the mine plant. This shall enlighten other operational optimization factors such as scaling and efficiency difference between dry and wet ball milling.

3.2 Results and Discussion

3.2.1 Further Laboratory Results and Discussion

Following the previous data from the laboratory experiments in Chapter 2, it can be observed from Figure 3-1 and Figure 3-2 that the lower process time and the higher the rpms, the more efficient the system is. On the other hand, this is equivalent to a variation in the number of revolutions, as observed in Figure 3-2b. Moreover, when analyzing the results obtained at fixed rpm values as illustrated in Figure 3-1b it is seen that the operating time again has a role on the exergy efficiency, with an associated and apparently linear increase in the energy consumption to perform the required comminution work, which would explain the decrease of efficiency.

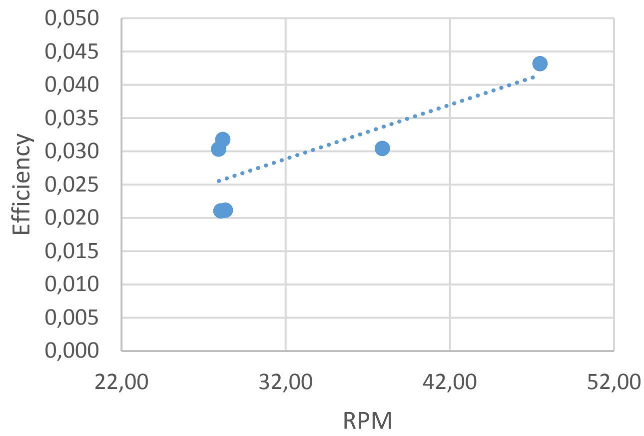

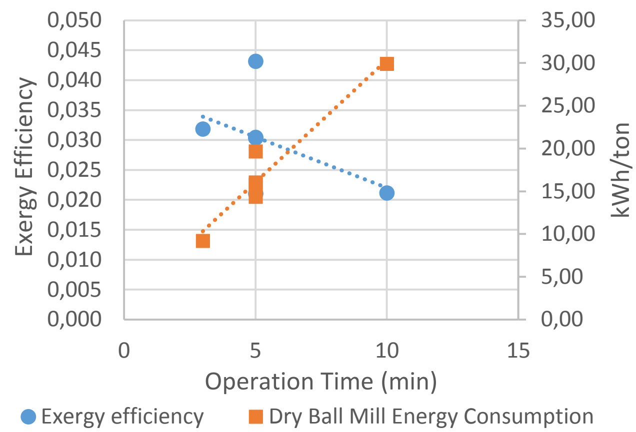

Figure 3-1 a) Exergy efficiency v/s rpm for dry ball mill. b) Exergy Efficiency and comminution work for 27-28 rpm dry ball mill

But if there is such an increase of energy consumption per unit of operation time, then shouldn't the particle size differences increase and therefore the efficiency should somehow stabilize or compensate this effect as seen in Table 2-5 and Table A-1 (annex)? The answer is yes, however this applies only if the ball milling process were entirely physically focused on comminution. From Figure 2-12 it is noted that most of the power consumed is mainly for the ball mill to turn when loaded and that the comminution process corresponds to a lesser part of the total ball mill work. This is also seen when comparing the machinery inertial minimum with the minimum practical energy for comminution. The ball mill normally turns with a nominal load inside of it, the extra material loaded is simply a marginal quantity of the original unloaded operational mass. Therefore, reviewing this new information, another efficiency improvement can be made by minimizing the comminution time at the optimal process speed to obtain a required ore size difference.

Furthermore, using the data plotted in Figure 3-3 a, b and c we have approximated contours of constant degree of grinding ($\Delta x/x$) and energy ball mill energy requirements (energy/mass). The grinding contour shown in Figure 3-3d was drawn to fit the data. The energy contour shown in Figure 3-3d was both drawn to fit the data and it is assumed that energy is proportional to RPM and time (*energy=A*RPM*t*, where *A* is a dimensionless constant). Figure 3-3d suggests that, for a given change in rock size, there maybe an optimum operating point on the RPM versus time curve to minimize energies. Significant further investigation is required in order to verify this.

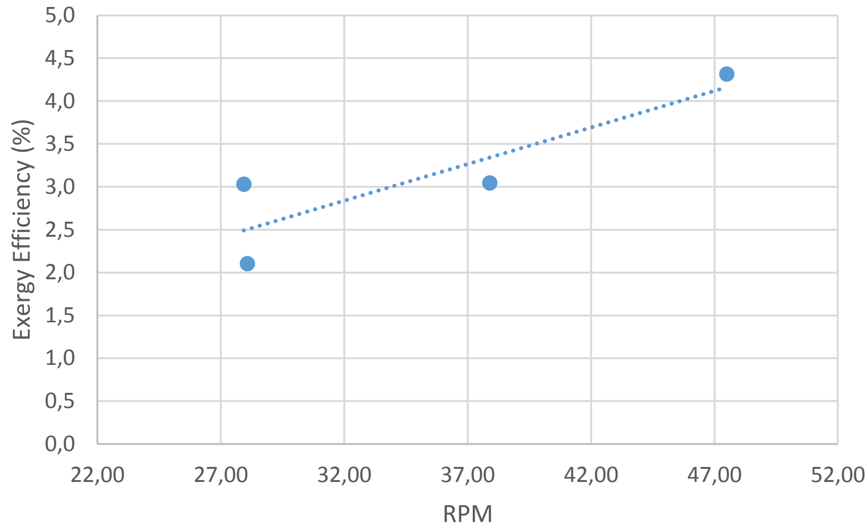

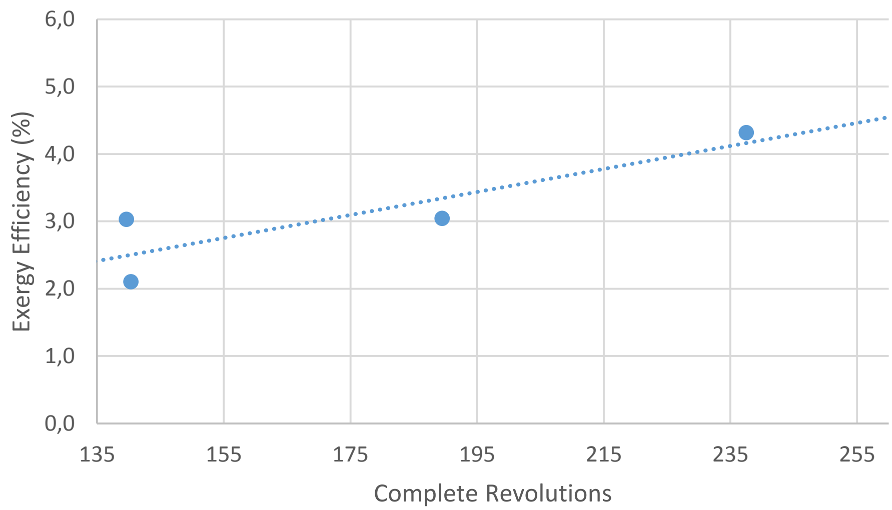

Figure 3-2 a) Exergy efficiency v/s RPM for samples at a fixed 5 minute operation time. b) Exergy efficiency v/s amount of revolutions made during the laboratory operation at a fixed 5 minute operation time

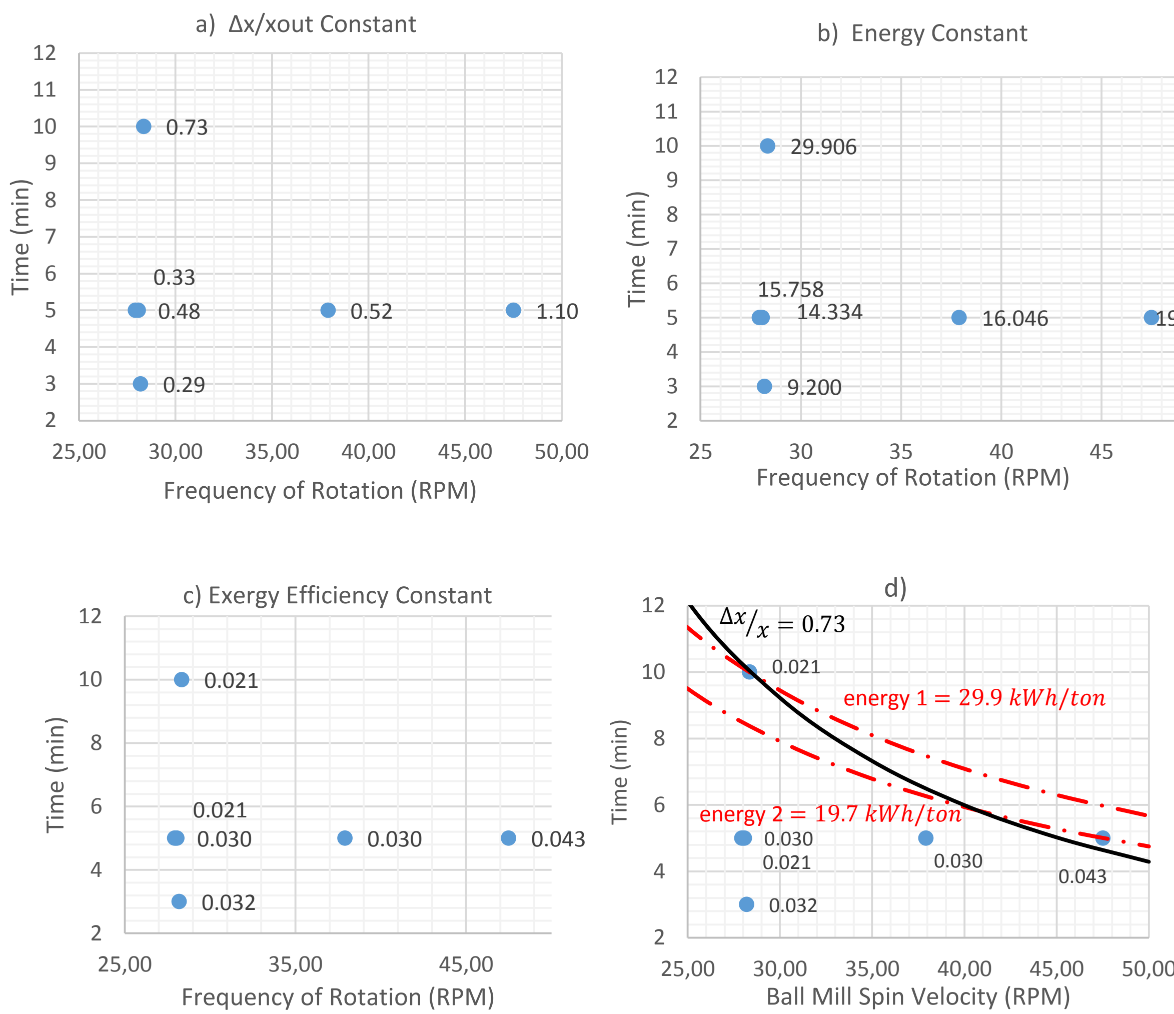

Figure 3-3 Operational curves in function of time and RPM with a) Δ grain size/outgoing grain size b) Energy consumed c) Exergy efficiency d) An operational example of the combination of the graph data

3.2.2 Mining Plant Results and Discussion

The material samples for both the laboratory from the preceding chapter and this section are from the same origin (the San Pedro Mining plant material during processing). Therefore the Hukki-Morrell relationship of minimum practical work and surface energy values of the material ore are equivalent for both studies.

a) Temperature rise effect

Measurement of the temperature was taken at different stages of the crushing and grinding process to develop an exergy assessment and localize main losses. These temperature measured correspond to the machinery shell, incoming feed and outgoing product for each stage, all shown in Figure 3-4.

At the first stage, there seems to be a major opportunity loss of the stored material rock heating up with the sun radiation. Although developing a system to capture this heat might influence the throughput of the process, there is a seemingly good opportunity in utilizing this energy. Even more if considering that the temperature difference of the stored rock and the incoming feed in the crusher is approximately 0.31kWh/ton (0.35kJ/kg) of energy which could be used in another process. For example, it is equivalent to a fifth of the energy consumed by the jaw crusher. This storage phase of the process in not included in the exergy efficiency assessment due to the selected control volume, although this improvement would increase the general exergetic efficiency of the mine plant as a whole.

Following the process flow, in the primary jaw crushing the losses of temperature through the shell seems to be high, although as seen in pictures taken form the plant (Figure A.1, annex), this must be due to the high exposure to solar radiation. This is confirmed when noticing the low temperature difference of incoming feed and outgoing product which is about 2ºC (15ºC lower than the shell temperature). On the other hand, the secondary and tertiary crushers don’t seem to have major temperature losses through the shell either but the material does also heat up 2-3ºC higher than the incoming feed temperature. It is in the wet ball mill where the highest temperature difference in the material is found. Therefore, at this phase the amount of retrievable energy should be highest. We shall review these opportunities further on with the exergy efficiency results.

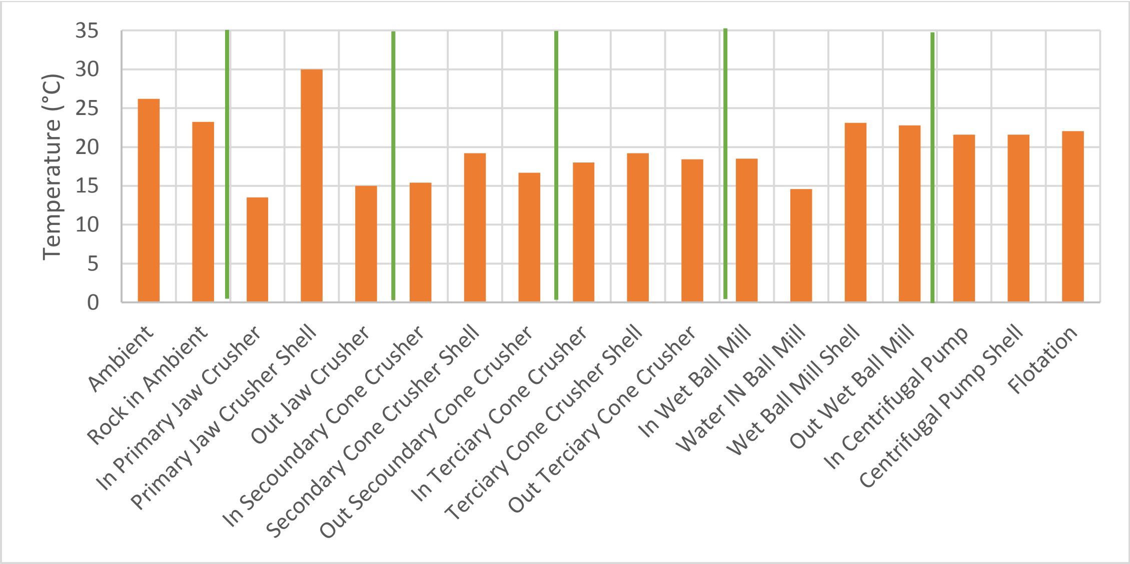

Figure 3-4 Temperature measurements made at the mining plant at the different stages.

On the other hand, the cooling oil in the cone crushers could also become an opportunity of optimization. As seen in Table 3-1, the cooling systems temperature of both crushers decreases a couple of degrees. This translates to an estimated 0.13kWh/ton (mass with respect of processed material) of average dissipated energy per cone crusher. This could be increased to a total of 0.87 kWh/ton (mass with respect of processed material) if the cooling oil heat at the tertiary cone crusher could be captured and brought down to ambient temperature. So, theoretically, if this heat energy could be captured and completely used as energy then the plant could save about 55.7% of the energy consumed by one of the cone crushers.

Table 3-1 Summary of cooling oil temperature and energy of cone crushers

	Secondary Cone Crusher	Tertiary Cone Crusher
Oil IN Machine Temperature (ºC)	26.6	28.7
Oil OUT Machine Temperature (ºC)	36.5	39
Estimated cooling energy kWh/ton (processed material)	0.123	0.143

b) Minimum comminution work

i) Data and boundary considerations

As explained in the previous chapter, it is important to keep in mind that this Hukki-Morrell relationship obtained by uniaxial compression tests will have a larger margin of error at each end of the process (jaw crushing and fine wet ball mill grinding) due to its distance from laboratory tested particle size range. Therefore, during this assessment we shall include results from a ubiquitous relationship as a general guideline as to verify the projected comminution energy for the particle size. We will use the Bond relationship as this alternative relationship guideline. In case the obtained Hukki-Morrell relationship error is too large, we shall use this ubiquitous relationship for that range instead. It is expected that the obtained Hukki-Morrell relationship should work 50% higher and a 50% lower (5850µm-950µm) from our laboratory testing. For simplicity, we will call this arbitrary margin the '50-50 criteria'.

For the inertial calculations, the relevant dimensions for the machinery are as follows. The primary jaw crusher, Figure 3-5 (I), is estimated as a solid thick heavy plate 25" wide (a.), 40" long (b.) and 11" thick (c.). The angular movement of the plate is estimated to be 0.29rad at 5Hz with the center of movement at the base of the plate. Both secondary and tertiary cone crushers Figure 3-5 (II) (same brand and model) are estimated to be a solid, 'non-tip', cone with initial radius 0.17m (d.), end radius 0.68m (e.), 0.48m high (f.) with a cylinder underneath of same end radius and 0.13m high (h). The cone crusher system was estimated to rotate at 100 rpm off centered by 0.15m from the vertical axis (i.). As for the ball mills, although the mine has various dimensions and brands, the dimensions were standardized to 1.8m of external diameter, 1.6m internal diameter, 3m long, loaded with 10.5 tons of 3” balls, a 10:1 ball to material load ratio, loaded to a 45% fill, rotating at 26 rpm. Equation (2.7) was applied again to estimate the inertial energy for the ball mill.

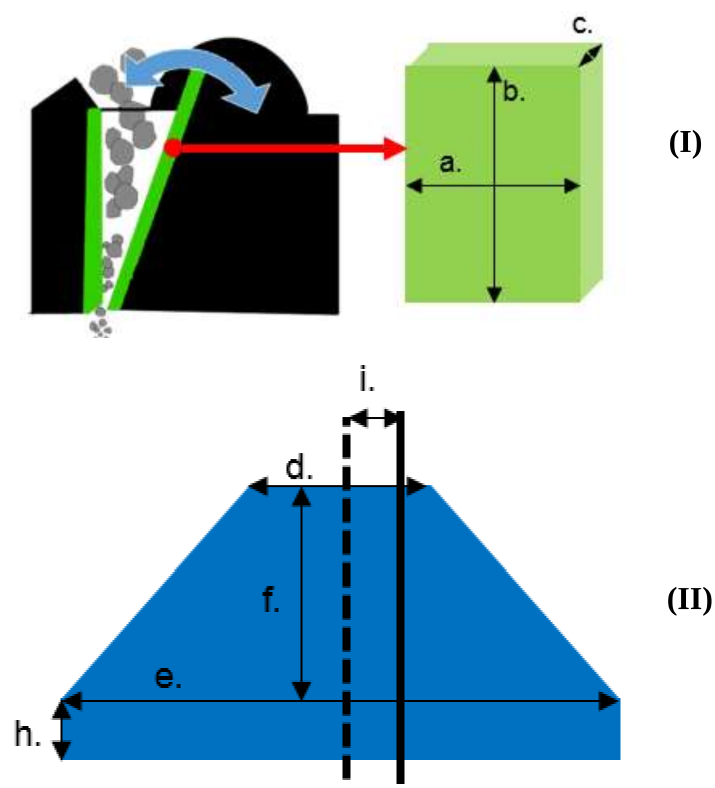

Figure 3-5 Illustration of the dimensions of the Primary Jaw Crusher (I) and the Secondary and Tertiary Cone Crusher (II)

The physical boundaries for the exergy balance rate utilized are similar to those of the previous assessment done to the laboratory ball mill, Figure 2-3, but applied to mine’s crushers and the ball mill’s geometry. Schematic drawing of the boundaries for the jaw and cone crushers are shown in Figure 3-6 where the outer dashes delimits the boundary where the material ore leaves and cools back down to ambient temperature, defined as BOUNDARY 1. The inner dots from Figure 3-6 delimit BOUNDARY 2 which considers the optimization case of which the heat of the material after comminution is saved and the destroyed exergy reduced. The ball mill schematic remains the same as in Figure 2-3. It is important to note that these assessments were made considering a dead state (the state in which the system reaches equilibrium with the environment) in the process flow utilizing data based on average measurements provided by the mining company ("Private conversations with Minera San Pedro," 2015).

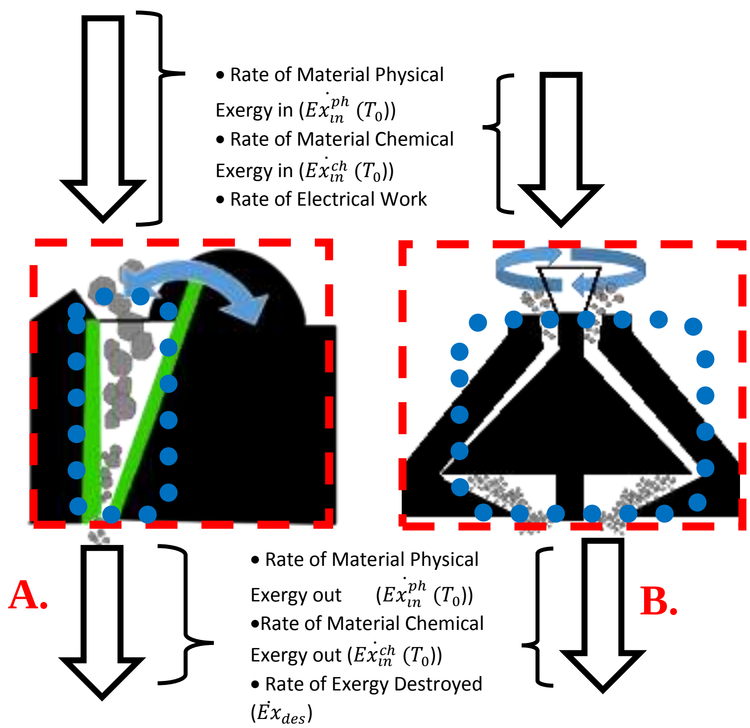

Figure 3-6 Jaw (a) and Cone (b) crusher energy and mass diagram

ii) Comminution minimum energy

A first reassurance obtained from Chapter 2 was the range in which our experimental Hukki-Morrell projection curve works correctly. As seen in Table A-2 (annex), comminution energy predicted by projections of our

Hukki-Morrell curve turn severely unrealistic for particle size ranges at the primary jaw crusher operation resulting in an projected energy consumption under the calculated surface energy difference which, as we will recall, is the theoretical minimum. Therefore, this linearity estimated by Morrell is only valid in the vicinity of the evaluated particle size. Perhaps, with the current data, a curve could be projectable to the further away size ranges but a linear behavior of the exponent cannot be taken as the relationship to accomplish this.

Moreover, considering this effect, it was noted that the secondary cone crusher energy results seems to be off when comparing with the ubiquitous relationship. But tertiary cone crusher and wet ball mill show reasonable results.

As stated before, it is reasonable to consider that the obtained Hukki-Morrell curve is adequate when considering the 50-50 criteria but it seems that, due to the low variation of comminution energy in the higher sized range particles (5850μm and larger), this upper limit could be extended up to the tertiary cone crusher particle feed size. As for the ball mill, for this study we shall also consider the obtained Hukki-Morrell relationship as a more conservative minimum work due to that the product size is also close to the limiting particle size (50-50 criteria).

Corrections such as to consider a complete Morrell relationship, Equation (1.3), was not possible. Although regression solutions resulted in a more precise value when varying the index as stated by Morrell, it was impossible to establish a clear relationship to model its behavior in the tested sized range for further projection of the relationship to other size ranges. Future research should look more into these relationships on a broader size range as to project comminution energy with a more precise relationship.

iii) Exergy results

The exergy analysis of the crushing and grinding phases of the plant using comminution minimum work are shown in the Grassmann and Sankey

Diagrams in Figure A.5 and Figure A.6 (annex). The same diagrams for exergy efficiency but considering machinery minimum work through machinery inertial calculation estimates were drawn in Figure A.7 (Annex). The full results of both assessments are shown in Table A-2 and a summary in Table 3-2.

In all Sankey and Grassmann graphs, energy flows are scaled to the amount of energy passing as to visually appreciate the amounts. Since surface energy is low compared with the other flows of energy and losses, we used separate scaling to appreciate this flow. In this case the average efficiency of the process using surface energy resulted to be a 1.11E-5%. In the Sankey diagram in Figure A.6 (annex) the minimum comminution energy flow is used as the practical minimum work to complete the process. On the other hand, the Sankey diagram in Figure A.7 (annex) illustrates the energy flow utilizing the minimum practical work of the machinery

Table 3-2 Summary of Exergy rate efficiency (in %).

Process	Jaw Crusher	Secondary Cone Crusher	Tertiary Cone crusher	Wet Ball Mill Grinding
Incoming T ºC	13.5	15.4	18	18.5
Outgoing T ºC	15	19.2	19.2	22.8
Incoming F80 (µm)	457200	74930	16640	3650
Outgoing P80 (µm)	74930	16640	3650	200
Electrical Work kWh/ton	1.56	1.56	2.74	14.67
Inertial Estimate kWh/ton	0.39	1.29	1.80	12.76
Comminution Work (Hukki-Morrell) kWh/ton	4.80E-07	0.09	1.19	2.42
Guideline Comminution Work (Bond) kWh/ton	0.36	0.68	1.46	8.99
Δ Physical Exergy kWh/ton	0.015	0.11	0.03	0.41
Efficiency B1 (%)	23.2	43.74	53.35	16.5
Efficiency B2 (%)	24.2	51.0	54.6	19.3
Inertial Efficiency (%)	24.95	82.29	65.6	87.02

Due to the fixed rpm of the plant's wet ball mill, an operational graph such as the one obtained previously in this chapter was not feasible to construct and the optimization of the exergetic efficiency based on this data could not be made. Although this is unfortunate for this evaluation, the practical application of this type of graphs for plant designing is high and encouraged for future studies.

Several results gave reassurances from Chapter 2: the low efficiency of the ball mill process for comminution, an adequate minimum practical work relationship is key for true energy efficiency assessment, and that heat energy savings from the material temperature rise is negligible.

This last conclusion was observed when calculating the efficiency of the different machinery in the second boundary where for example in the ball mill resulted to be an increase of efficiency of 2.8%. This efficiency increase is equivalent to 0.41kWh/ton savings, similar to what could have been obtained by recapturing heat from the rocks stored before the primary jaw crusher and less than half of the energy that could be recaptured from the cooling oil from the cone crushers.

Moreover, although the comminution efficiency of the wet ball mill is low, 16.5%, it is still an order of magnitude higher that what was obtained on the laboratory scale ball mill. This is thought to be given by three factors: (i) the higher potential energy the balls have when rotating in ball mills with higher diameter; (ii) that the ratio of material, water and chemicals enhance the conversion of energy compared to a dry ball mill; and (iii) a better selection of the operational gear box and electrical motor.

The first statement is related to when the ball mill has a larger diameter, the fall height increases (more potential energy), therefore the energy transfer from the ball to the material ore is higher (due to the higher kinetic energy that can be achieved), and therefore the rock is grinded into a lower grain size with a lower amount of impacts.

The second statement is a technicality concerning the boundary of the balance rate and also another reason why energy assessment including balance rates of different substances, help narrow down parameters that help optimization. Since the power of the motors has to be divided by the material flow, strictly speaking the material flow is the sum of the ore and the liquid aggregates processed in the ball mill. But if this were to be divided only by the material ore, as would a dry ball mill process, then the electric motor specific work (per mass) would be higher and the efficiency drops to a 5.21% (or an 6.1% if the materials heat were to be recaptured).

The third statement is highly related to the discussion done on Figure 2-12 from Chapter 2. It is possible that the higher efficiency is due to a higher quality transmission system, a better motor selection to operate the process in which heat losses are therefore a much lesser fraction of the total losses. This would require more research for confirmation.

iv) Machinery practical minimum work

Utilizing the inertial machinery minimum energy as the incoming energy or, in other words, to consider that the energy consumed by the machinery is at its maximum efficiency considering the nature of the system, results in that the wet ball mill comminution energy efficiency is of an 18.97%. This means that the process will be always inefficient regardless of optimization efforts. Jaw and cone crushers on the other hand seem to be efficient under this same scope resulting in a 70.6% on average. This average can be separated into a 93.04% for jaw crushing, 52.8% and 66.1% for secondary and tertiary cone crushers and an 18.9% for the wet ball milling. These results show that the most efficient process, only in theory, is the jaw crusher and the least to be the wet ball mill.

On the other hand, utilizing the inertial machinery minimum energy as the minimum work for comminution results in that the ball mill has an efficiency of 87% which is much better than what was obtained from the laboratory ball mill. This means that, considering the machinery applied, the plant’s ball mill is fairly efficient which could be due to a simpler torque converter (motor to drum), a better selected motor and operational parameters. Although this also means that there is little room for improvement if a comminution efficiency were to be considered. Moreover, the only way to make a considerable change would be to increase the throughput of the process. For example, when increased to 100ton/hr, the comminution efficiency increases to a 53%. Therefore, it can be stated that ball milling *per se* is an inefficient process although it is at the current time one of the best methods to perform fine grinding with the highest throughput.

As a side note, another scaling factor related with inertial calculations which is interesting to review is the percent of energy from ball and material load torque and the inertial rotation of the drum of the ball mill when calculating machinery inertial minimum energy. Recalling the previous Chapter, the laboratory dry ball mill consumed nearly 92.7% of its energy in the torque due to the weight of the balls. In wet ball milling on the other hand, this is more balanced resulting in a calculated consumption of 50.2% in the material and ball load and a 49.8% with regard of inertial rotation of the drum.

3.3 Main Conclusions

The study research achieved several findings. The first and foremost is the capability of determining the minimum practical comminution work with uniaxial compression testing and utilizing the Hukki-Morrell relationship curve. This gives an advantage for engineers to assess mine plants due to that it is a simpler, lower cost and practical way to determine minimal energy although it is important for engineers to keep in mind its limitations. It is less precise than considering surface energy, but the latter, although theoretically rigorous for studying ideal processes, it is unpractical for aiding industrial assessment due its extremely low value. But it is also important to keep in mind that the Hukki-Morrell relationship derivation through uniaxial compression highly depends of the machines capacity to compress and therefore must be studied throughout the assessed range or as close as possible. Moreover, considering a single local linearity of the exponent with a fixed index does not provide an adequate projection for much larger particle sizes. Local determination of the index function with respect of grain size is insufficient to determine a relationship. Therefore, it is suggested to perform tests as to adjust the parameters and carry out a better assessment.

Energy saved by heat capturing represents about a 2.8% of an operation efficiency increase for ball mill grinding operations. This low improvement is due to the low temperature difference in income and outcome heat of the material as they are close to the reference point, the ambient temperature. Although on the other hand, by recapturing heat that leaves the cone crushers through refrigerant oils or to use the accumulated heat from the stored rocks, one could retrieve energy which is not being used and apply it on another process. This should be further reviewed by the mining plant due to that it would mean not only an increased overall efficiency but also savings in operational costs.

Another difference in energy efficiency relies on wet vs dry ball milling. This difference is, as discussed before, the specific energy (per mass) consideration from the selected boundary, emphasizing again on the importance of determining boundaries correctly and the utility of assessing when boundaries are modified.

Adequate electric motor and transmission system selection and maintenance are also important factors for optimizing the energy. Both should be studied on each case for an adequate operation and desired optimal operation standards, as well as to be considered for future research and development. Although ball milling itself is an inefficient process for performing comminution, it can be improved when utilizing the correct equipment.

3.4 Further Research

This research has covered several topics that would be interesting to research further. Comminution theory, although thoroughly studied, has not given into a practical minimum work method that truly represents the comminution minimum energy. The ball mill process is a largely inefficient process and, when compared with an optimized ball mill, it does not provide a practical minimum work for comminution. On the other hand, while uniaxial compression gives a lower energy result for comminution, it lacks the kinetic energy which also is involved in the process. Therefore, a weighing study of these two factors for different scale processes would help on this practical work determination.

On the other hand, energy savings rely on the recapturing of the heat leaving the system through the shell or machinery. As shown before, the material does not draw much heat energy and most of the heat losses leave through the shell. The sum of these losses gives into account energy savings enough to run freely some of the machinery of the mining process. Therefore, utilization of these losses should be researched. Another possibility, although already researched, is the optimization of the ball diameters, material load, ball to mass ratio and liner design to improve the efficiency.

Moreover, this study calls for research on adequate motor sizing and transmission system optimization for machinery and the development of optimization curves such as proposed in Figure 3-3. This type of graph should become useful for plant designing, giving the operator the flexibility on choosing the operation parameters and determining the efficiency rapidly.

On the other hand, there are studies which correlate the most efficient separate components of the machine available to the market with the current machinery as to obtain an actual and to date efficiency measurement (Schudeleit, Züst, & Wegener, 2015; Schudeleit, Züst, Weiss, & Wegener, 2016). In other words, the method reviews for example the best electric motor, power transmission system, bearings, etc. and compares them with the assessed machinery. It would be interesting to establish a reference point of the plant's efficiency in comparison with the market.

Finally, although the exergy assessment was made for the crushing and grinding of the copper mining process, it would also be interesting to revise the flotation and lixiviation of the copper ore and research different sensibilities and optimization variables to improve in the process.

BIBLIOGRAPHY

Alvarado, S., Alguerno, J., Auracher, H., & Casali, A. (1998). Energy and Exergy Optimization of Comminution. *Energy*, *23*(2), 153–158.

Bai, Y., He, F., Fu, B., & Han, X. (2014). Energy Calculation Model of ball kinematics based on ball mill coal load. *International Journal of Innovative Computing, Information and Control*, *10*(5), 1715–1725.

Bakshi, B. R., Gutowski, T. G., & Sekulic, D. P. (2011). *Thermodynamics and the Destruction of Resources*. Cambridge University Press. http://doi.org/10.1017/CBO9780511976049

Ballantyne, G. R., & Powell, M. S. (2014). Benchmarking comminution energy consumption for the processing of copper and gold ores. *Minerals Engineering*, *65*, 109–114. http://doi.org/10.1016/j.mineng.2014.05.017

Biolin Scientific. (2016). Surface free energy - theory and calculations. Retrieved March 3, 2016, from http://www.biolinscientific.com/zafepress.php?url=/pdf/Attension/Theory Notes/AT_TN_4_sfe.pdf

Bond, F. C. (1952). Bond-ThirdTheoryofComminution.pdf, *193*, 484–494. Retrieved from http://www.ewp.rpi.edu/hartford/~ernesto/S2014/SHWPCE/Papers/SW-Preprocessing-Separation-Recycling/Bond-ThirdTheoryofComminution.pdf

Bond, F. C. (1961). *Crushing and grinding calculations*. Allis-Chalmers Manufacturiing Company.

Bueno, M., Foggiatto, B., & Lane, G. (2015). Geometallurgy Applied in Comminution To Minimize Design Risks, *4101*, 1–19.

Clausius, R. (1879). *The mechanical theory of heat*. Macmillan.

Cleary, P. W. (2001). Charge behaviour and power consumption in ball mills: Sensitivity to mill operating conditions, liner geometry and charge composition. *International Journal of Mineral Processing*, *63*(2), 79–114. http://doi.org/10.1016/S0301-7516(01)00037-0

Comisión Chilena del Cobre. (2015). Inversión en la minería chilena - Cartera de proyectos 2014 -2023 - Informe_de_Consumo_de_Energia_2014_VF.pdf. Retrieved November 30, 2015, from http://www.cochilco.cl/descargas/estudios/informes/energia/Informe_de_Consumo_de_Energia_2014_VF.pdf

Das, A., Nguyen, G. D., & Einav, I. (2013). The propagation of compaction bands in porous rocks based on breakage mechanics. *Journal of Geophysical Research: Solid Earth*, *118*(5), 2049–2066. http://doi.org/10.1002/jgrb.50193

Davis, E. W. (1919). Fine crushing in ball mills. *Trans. AIME*, *61*, 250.

Dong, H., & Moys, M. H. (2003). Load behavior and mill power. *International Journal of Mineral Processing*, *69*(1-4), 11–28. http://doi.org/10.1016/S0301-7516(02)00046-7

Douillard, J. M., Salles, F., Henry, M., Malandrini, H., & Clauss, F. (2007). Surface energy of talc and chlorite: Comparison between electronegativity calculation and immersion results. *Journal of Colloid and Interface Science*, *305*(2), 352–360. http://doi.org/10.1016/j.jcis.2006.08.010

Forssberg, E., & Pourghahramani, P. (2005). Mineral Processing and Extractive Metallurgy Review : REVIEW OF APPLIED PARTICLE SHAPE DESCRIPTORS AND PRODUCED PARTICLE SHAPES IN GRINDING ENVIRONMENTS . PART II : THE INFLUENCE OF COMMINUTION ON THE PARTICLE SHAPE. *Mineral Processing and Extractive Metallurgy*, *26*, 167–186. http://doi.org/10.1080/08827500590912103

Gibbs, J. W. (1879). On the Equilibrium of Heterogeneous Substances. *Trasnactions of the Conneticut Academy of Arts and Sciences*, *III*, 343–524.

Guillard, F., Golshan, P., Shen, L., Valdes, J. R., & Einav, I. (2015). Dynamic patterns of compaction in brittle porous media. *Nature Physics*, *11*(10), 835–838. http://doi.org/10.1038/nphys3424

Gupta, C. K. (2003). *Chemical Metallurgy Principles and Practice*.

Haffez, G. S. A. (2012). CORRELATION BETWEEN BOND WORK INDEX AND MECHANICAL PROPERTIES OF SOME SAUDI ORES 1- INTRODUCTION. *Journal of Engineering Sciences*, *40*(1), 271–280.

Hogg, R., & Fuerstenau, D. W. (1972). Transverse mixing in rotating cylinders. *Powder Technology*, *6*(3), 139–148. http://doi.org/10.1016/0032-5910(72)80070-6

Hukki. (1962). Proposal for a Solomonic Settlement Between. *AIME Transactions*.

Instituto Nacional de Estadísticas Chile. (2013). *Compendio Estadístico 2013*.

Issen, K. A., & Rudnicki, J. W. (2001). Theory of compaction bands in porous rock. *Physics and Chemistry of the Earth, Part A: Solid Earth and Geodesy*, *26*(1-2), 95–100. http://doi.org/10.1016/S1464-1895(01)00031-X

Kapur, P. C., & Fuerstenau, D. W. (1987). Energy-size reduction "laws" revisited. *International Journal of Mineral Processing*, *20*(1-2), 45–57. http://doi.org/10.1016/0301-7516(87)90016-0

Karunatilake, N., Kuhn, P., Matei, I., Munasinghe, J., Seibold, B., Surajiyono, … Döfler, W. (2000). *Dynamics of Balls and Liquid in a Supervisor :*

Kick, F. (1885). *Das Gesetz der proportionalen Widerst{ä}nde und seine Anwendungen: Nebst Versuchen {ü}ber das Verhalten verschiedener Materialien bei gleichen Form{ä}nderungen sowohl unter der Presse als dem Schlagwerk*. A. Felix. Retrieved from https://books.google.cl/books?id=yKtLAAAAMAAJ

King, R. P. (2000). TECHNICAL NOTES 8 GRINDING.

Krüss GmbH. (2016). Surface free energy. Retrieved March 3, 2016, from http://www.kruss.de/services/education-theory/glossary/surface-free-energy/

Lynch, A. J. (1977). Mineral crushing and grinding circuits. *Developments in Mineral Processing*, *1*, 195–225. http://doi.org/10.1080/10643389.2012.728825

Lynch, A. J., & Rowland, C. A. (2005). *The History of Grinding*. Society for Mining, Metallurgy, and Exploration. Retrieved from https://books.google.cl/books?id=Kj7PSOqTZ3IC

Magdalinovic, N., Trumic, M., Trumic, M., & Andric, L. (2012). The optimal ball diameter in a mill. *Physicochemical Problems of Mineral Processing*, *48*(2), 329–339. http://doi.org/10.5277/ppmp120201

Marshall, D. M., Barnhart, R. K., Shappee, E., & Most, M. T. (2015). *Introduction to Unmanned Aircraft Systems, Second Edition*. Taylor & Francis. Retrieved from https://books.google.cl/books?id=pZhBBAAAQBAJ

Mattew, C. (2010). *Adhesion and the surface energy components of natural mineral and aggreates*.

Metso. (2010). *Basics in minerals processing*.

Miller, J. D., Young, C., Kellar, J. J., & Free, M. L. (2005). *Innovations in Natural Resource Processing: Proceedings of the Jan. D. Miller Symposium*. Society for Mining, Metallurgy, and Exploration, Incorporated. Retrieved from https://books.google.cl/books?id=rktcHNr3q-4C

Mio, J. K. H., Saito, F., & Miyazaki, M. (2001). CORRELATION OF GRINDING RATE OF GIBBSITE WITH IMPACT ENERGY IN TUMBLING MILL WITH MONO-SIZE BALLS Mill diameter Milllength Critical rotational speed Median diameter of original sample Sample weight Grinding time, *14*(10), 1213–1223.

Mishra, B. K., & Thornton, C. (2002). An improved contact model for ball mill simulation by the discrete element method. *Advanced Powder Technology*, *13*(1), 25–41. http://doi.org/10.1163/15685520252900938

Monov, V., Sokolov, B., & Stoenchev, S. (2012). Grinding in ball mills: Modeling and process control. *Cybernetics and Information Technologies*, *12*(2), 51–68.

Morrell, S. (2004). An alternative energy–size relationship to that proposed by Bond for the design and optimisation of grinding circuits. *International Journal of Mineral Processing*, *74*(1-4), 133–141. http://doi.org/10.1016/j.minpro.2003.10.002

Mular, a. L. (1965). Comminution in Tumbling Mills: A Review. *Canadian Metallurgical Quarterly*, *4*(1), 31–74. http://doi.org/10.1179/000844365795164963

Musa, F., & Morrison, R. (2009). A more sustainable approach to assessing comminution efficiency. *Minerals Engineering*, *22*(7-8), 593–601. http://doi.org/10.1016/j.mineng.2009.04.004

Mwanga, A. (2014). *Test Methods for Characterising Ore Comminution Behavior in Geometallurgy*. Retrieved from https://pure.ltu.se/portal/files/96464806/Abdul_Mwanga.pdf

Petela, R. (1984). Exergetic efficiency of comminution of solid substances, *63*, 414–418.

Private conversations with Minera San Pedro. (2015). In *Minera San Pedro Report Data*.

Rasband, W. (2015). ImageJ 1.48V. National Insitutes of Health, USA. Retrieved from http://imagej.nin.gov

Rittinger, Pr. (1867). *Lehrbuch der Aufbereitungskunde*. Berlin.

Rose, H. E., & Sullivan, R. M. E. (1958). *A treatise on the internal mechanics of ball, tube, and rod mills*. Constable.

Rosen, M. a., Dincer, I., & Kanoglu, M. (2008). Role of exergy in increasing efficiency and sustainability and reducing environmental impact. *Energy Policy*, *36*(1), 128–137. http://doi.org/10.1016/j.enpol.2007.09.006

Sahoo, A. (2014). Simulation studies on Energy Requirement , Work Input and Grindability of Ball Mill, *4*(2).

Schudeleit, T., Züst, S., & Wegener, K. (2015). Methods for evaluation of energy efficiency of machine tools. *Energy*, *93*, 1964–1970. http://doi.org/10.1016/j.energy.2015.10.074

Schudeleit, T., Züst, S., Weiss, L., & Wegener, K. (2016). The Total Energy Efficiency Index for machine tools. *Energy*, *102*, 682–693. http://doi.org/10.1016/j.energy.2016.02.126

SERNAGEOMIN Chile. (2015). *Catastro de depósitos de relaves*. Retrieved from http://www.americanbanker.com/issues/179_124/which-city-is-the-next-big-fintech-hub-new-york-stakes-its-claim-1068345-1.html

Stamboliadis, E. T. (2007). The energy distribution theory of comminution specific surface energy, mill efficiency and distribution mode. *Minerals Engineering*, *20*(2), 140–145. http://doi.org/10.1016/j.mineng.2006.07.009

Szargut, J., Morris, D. R., & Steward, F. R. (1987). Exergy analysis of thermal, chemical, and metallurgical processes.

Tangsathitkulchai, C. (2003). The effect of slurry rheology on fine grinding in a laboratory ball mill, *69*, 29–47.

Tromans, D. (2008). Mineral comminution: Energy efficiency considerations. *Minerals Engineering*, *21*(8), 613–620. http://doi.org/10.1016/j.mineng.2007.12.003

United States Geological Survey. (2011). Estimates of Electricity Requirements for the Recovery of Mineral Commodities , with Examples Applied to Sub-Saharan Africa, 100.

von Helmholtz, H. (1882). *Die thermodynamik chemischer Vorg{ä}nge*.

Yavuz, H., Altindag, R., Sarac, S., Ugur, I., & Sengun, N. (2006). Estimating the index properties of deteriorated carbonate rocks due to freeze–thaw and thermal shock weathering. *International Journal of Rock Mechanics and Mining Sciences*, *43*(5), 767–775. http://doi.org/10.1016/j.ijrmms.2005.12.004

Zang, L. (2013). Lecture 8 : Surface tension , internal pressure and energy of a spherical particle or droplet. Salt lake City: College of Engineering, University of Utah. Retrieved from http://www.eng.utah.edu/~lzang/images/lecture-8.pdf

Zhao, Y. (2014). Brief Talk about the Application and Development of Coal Mine

Machinery. In *3rd International Conference on Science and Social Research* (pp. 1330–1333).

A N N E X

ANNEX A: DRY BALL MILL EXERGY FLOW ASSESMENT

Table A-1 Dry Ball Mill Exergy Flow Assessment

	Unit	Lab 1	Lab 2	Lab 3	Lab 4	Lab 5	Lab 6
Passing 80% Feed size (f80)		**3900**	**5840**	**5840**	**5840**	**5840**	**5840**
Passing 80% Product size (p80)		**2643.10**	**4542.47**	**4392.91**	**3381.94**	**2785.23**	**3838.05**
Average Feed size		**3680**	**5180**	**5180**	**5180**	**5180**	**5180**
Average Product size		**1913.05**	**3635.27**	**3078.29**	**2017.51**	**1838.81**	**2426.47**
Temp Mat in	**C**	**16.1**	**14.2**	**14**	**13.9**	**12.8**	**13.5**
Temp Mat out	**C**	**17.7**	**14.9**	**14.6**	**16.3**	**14.2**	**15.4**
Temp Amb	**C**	**17.9**	**15.3**	**14.4**	**15.8**	**14**	**15**
Time	**hh:mm:ss**	**0:05:00**	**0:03:00**	**0:05:00**	**0:10:00**	**0:05:00**	**0:05:00**
Flows							
MINERALS IN	kg/hr	131.69	199.60	119.87	59.64	119.96	119.69
MINERALS OUT	kg/hr	131.69	199.60	119.87	59.64	119.96	119.69
1st Law							
U MIN IN	kWh/ton	24.27	24.08	24.06	24.05	23.95	24.02
MEC WORK	kWh/ton	14.33	9.20	15.76	29.91	19.65	16.05
BOND WORK	kWh/ton	0.571	0.291	0.332	0.682	0.973	0.507
Compression H-M Work p80	kWh/ton	0.43	0.29	0.33	0.63	0.85	0.49
Inertial Minimum	kWh/ton	1.84	1.25	1.79	2.93	3.13	2.48
H MIN OUT	kWh/ton	24.42	24.15	24.12	24.29	24.08	24.20
Surface Energy Minimum	kWh/ton	2.8E-14	4.14E-14	4.77E-14	1.06E-13	1.59E-13	7.57E-14
2nd Law							
S MIN IN	kWh/ton	-0.15	-0.09	-0.03	-0.16	-0.10	-0.13
EXERGY MIN IN	kWh/ton	24.65	24.41	24.33	24.45	24.28	24.37
S MIN OUT	kWh/ton	-0.02	-0.03	0.02	0.04	0.02	0.03
EXERGY MIN OUT	kWh/ton	24.67	24.42	24.34	24.48	24.30	24.40
DELTA EXERGY	kWh/ton	0.02	0.01	0.01	0.03	0.02	0.03
CHEMICAL EXERGY	kWh/ton	0.23	0.23	0.23	0.23	0.23	0.23

Efficiency	**Exergy Boundary 1 (Hukki)**	**0.0303**	**0.0318**	**0.0210**	**0.0212**	**0.0432**	**0.0304**
	Exergy Boundary 1 (Surface Energy)	**1.95E-15**	**4.50E-15**	**3.03E-15**	**3.54E-15**	**8.08E-15**	**4.72E-15**
	Exergy Boundary 2	**0.0318**	**0.0328**	**0.0216**	**0.0223**	**0.0441**	**0.0320**
	Bond Boundary 1	**0.0398**	**0.0316**	**0.0211**	**0.0228**	**0.0495**	**0.0316**
	Inertial	**0.1641**	**0.1641**	**0.1641**	**0.1641**	**0.3556**	**0.2669**
	Transit	**64.70**	**72.73**	**60.89**	**45.92**	**56.79**	**60.94**

ANNEX B : EXERGY RATE BALANCE FOR MINERA SAN PEDRO´S CRUSHING AND GRINDING

MASS BALANCE (dm)							
		JAW CRUSHER	SECONDARY CONE CRUSHER	TERTIARY CONE CRUSHER	BALL MILL		
MINERALS IN	ton/hr	60.00	60.00	60.00	MINERALS IN	12.5	t/hr
MINERALS OUT	l/hr	60.00	60.00	60.00	WATER IN	25	t/hr
					Recirculation	2	t/hr
					BALLS IN	0.0013	t/hr
					LINER IN	0.0815	t/hr
					MINERALS OUT	39.5829	t/hr

FIRST LAW (ENERGY)							
		JAW CRUSHER	SECONDARY CONE CRUSHER	TERTIARY CONE CRUSHER	BALL MILL		
ENTHALPY MINERAL IN	kWh/ton	24.02	24.22	24.46	H MINERAL IN	24.51	kWh/ton
ENTHALPY MINERAL OUT	kWh/ton	24.17	24.33	24.50	H H20 IN	16.33	kWh/ton
MECHANICAL WORK	kWh/ton	1.56	1.56	2.74	MECHANICAL WORK	14.67	kWh/ton
BOND WORK	kWh/ton	0.36	0.68	1.46	BALLS IN	33.52	kWh/ton
HUKKI WORK	kWh/ton	4.80E-07	0.09	1.19	Hukki Work	2.42	kWh/ton
SURFACE ENERGY WORK	kWh/ton	6.79E-07	1.25E-08	6.27E-10	Surface Energy	7.02E-10	kWh/ton
INERTIAL WORK	kWh/ton	0.39	1.29	1.80	Liner IN	32.63	kWh/ton
					Inertial	12.76	kWh/ton
					BOND WORK	8.99	kWh/ton
					H MINERAL OUT	19.07	kWh/ton

FIRST+SECOND LAW							
		JAW CRUSHER	SECONDARY CONE CRUSHER	TERTIARY CONE CRUSHER	BALL MILL		
Entropy Mineral IN	kWh/ton	-1.08	-0.92	-0.70	S MIN IN	-0.65	kWh/ton
EXERGY MIN IN	kWh/ton	25.46	25.37	25.39	S H20 IN	-0.33	kWh/ton
Entropy Mineral OUT	kWh/ton	-0.95	-0.81	-0.66	S MINRE IN	-0.88	kWh/ton
Exergy Mineral OUT	kWh/ton	25.35	25.26	25.35	S LINERS IN	0.00	kWh/ton
Chemical Exergy	kWh/ton	0.23	0.23	0.23	S BALLS IN	0.00	kWh/ton
Exergy destroyed	kWh/ton	1.23	1.02	1.99	EXERGY MIN IN	25.16	kWh/ton
					EXERGY H20 IN	16.66	kWh/ton
					EXERGY MINRE IN	19.95	kWh/ton
					EXERGY LINER IN	32.63	kWh/ton
					EXERGY BALLS IN	33.52	kWh/ton
					S MIN OUT	-0.88	kWh/ton
					EXERGY MIN OUT	19.95	kWh/ton
Exergy efficiency B1 Hukki		3.09E-07	0.057	0.433	Ex efficiency B1 H	0.165	
Exergy efficiency B1 Bond		0.2320	0.4374	0.5335	Ex efficiency B1 B	0.61	
Exergy efficiency Surface Energy		4.36E-07	8.05E-09	2.29E-10	Ex efficiency Surface Energy	4.79E-11	
Ex efficiency B2		0.242	0.510	0.546	Ex efficiency B2	0.193	
Inertial Efficiency		0.249	0.829	0.656		0.87	

Table A-2 Exergy rate balance for Minera San Pedro's crushing and grinding

ANNEX C: PICTURES OF THE DIFFERENT STAGES OF CRUSHING AND GRINDING AT THE SAN PEDRO MINING PLANT

Figure A.1 Primary Jaw Crusher

Figure A.2 (In Picture) Tertiary cone crusher. Secondary cone crusher is similar.

Figure A.3 Two of a total of three ball mills

Figure A.4 Flotation tanks

ANNEX D: GRASSMANN DIAGRAM FOR MINERA SAN PEDRO´S CRUSHING AND GRINDING IN kWh/ton

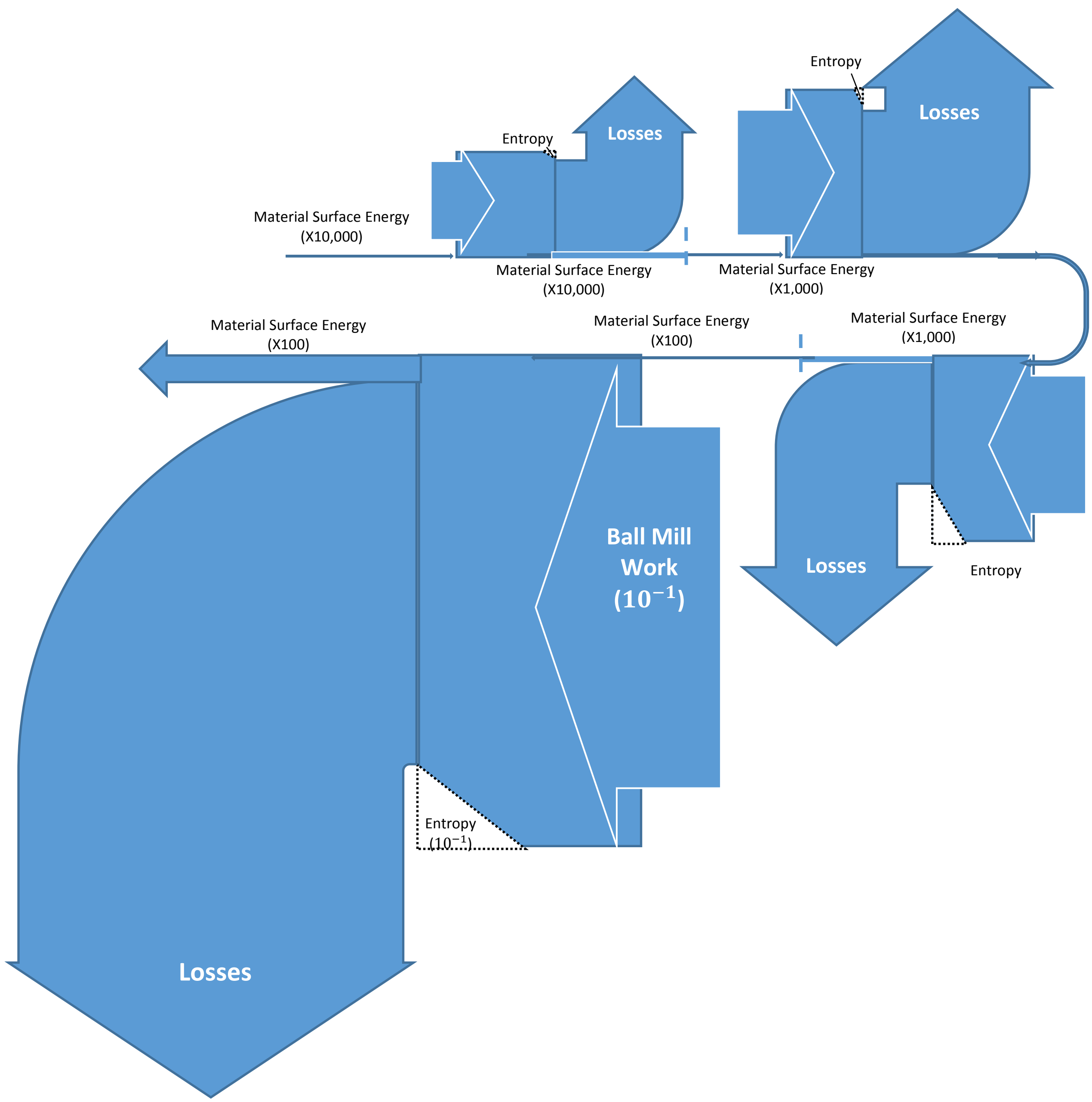

Figure A.5 Grassmann Diagram for Minera San Pedro's crushing and grinding in kWh/ton

ANNEX E : SANKEY DIAGRAM FOR MINERA SAN PEDRO´S CRUSHING AND GRINDING IN kWh/ton

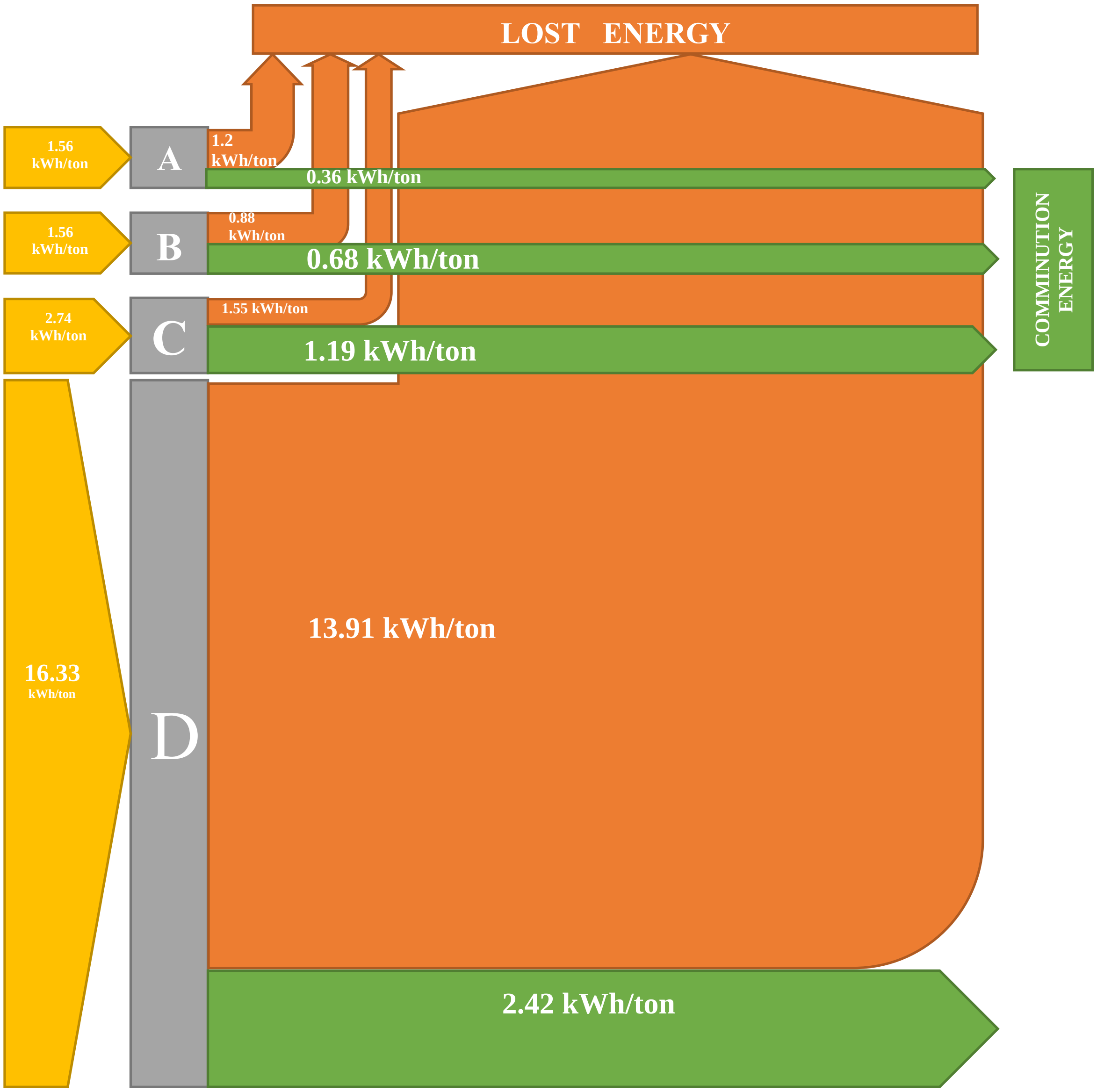

Figure A.6 Sankey Diagram for Minera San Pedro's crushing and grinding in kWh/ton using comminution minimum energy. A) Primary jaw crusher B) Secondary cone crusher C) Tertiary cone crusher D) Wet ball mill

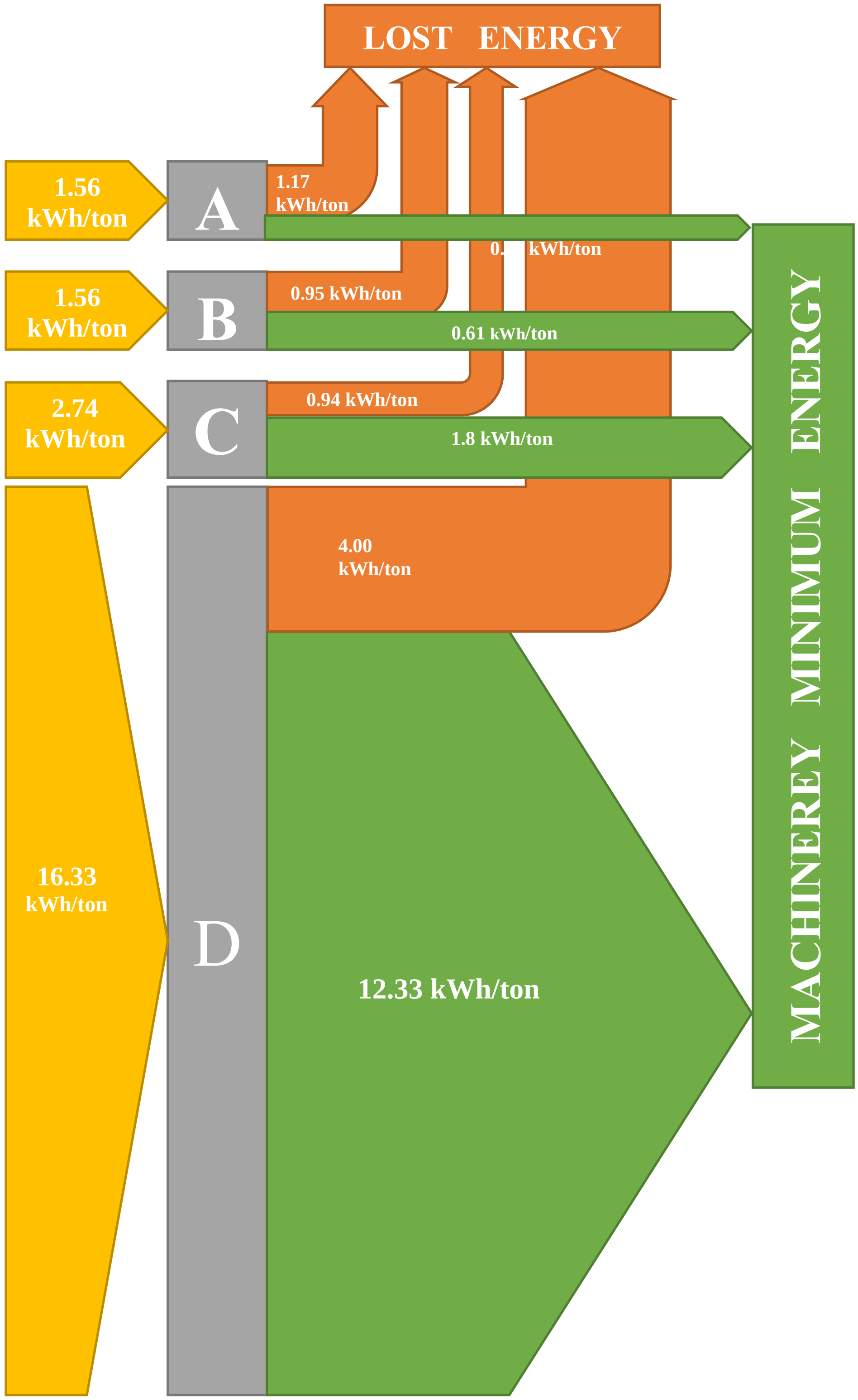

Figure A.7 Sankey Diagram for Minera San Pedro's crushing and grinding in kWh/ton using machinery minimum energy. A) Primary jaw crusher B) Secondary cone crusher C) Tertiary cone crusher D) Wet ball mill

ANNEX F : DATA RESULTS FROM UNIAXIAL COMPRESSION TESTING

Table A-3 Data Results from uniaxial compression testing.

	Test 01	Test 02	Test 03	Test 04	Test 05	Test 06	Test 07	Test 08	Test 09	Test 10	Test 11	Test 12
6000-4000 µm	0	0	0	0	0	0	0	0	0	0	3.87	1.04
4000-3350 µm	9.23	19.03	7.95	22.79	8.6	5.27	6.49	9.35	5.49	1.51	10.49	2.91
3350-2360 µm	11.43	9.04	11.24	5.56	11.97	9.91	10.09	6.06	7.25	2.75	3.74	5.6
2360-1700 µm	3.72	0.97	4.4	0.71	4.28	6.1	5.48	2.59	3.57	4.95	1.24	3.88
1700-850 µm	2.75	0.42	2.78	0.45	2.91	4.29	4.11	1.47	2.3	5.75	0.65	3.55
850-600 µm	0.78	0.13	0.9	0.12	0.82	1.33	1.06	0.42	0.54	1.44	0.21	1.01
under 600 µm	2.05	0.35	2.16	0.21	1.87	3.36	3.1	0.81	1.43	3.83	0.53	2.63
Displacement	2.49	1.5	2.99	1	1.99	2.49	2.49	1.5	2	2.7	2	3
Weight (g)	29.96	29.94	29.43	29.84	30.45	30.26	30.33	20.7	20.58	20.23	20.73	20.62
Work (J)	12.845	2.064	14.323	1.227	10.842	20.955	20.084	10.630	11.271	32.620	4.523	19.639
Power (W)	0.026	0.005	0.020	0.003	0.018	0.028	0.027	0.023	0.019	0.040	0.008	0.022

ANNEX G: DATA RESULTS FROM DRY BALL MILL TESTING

Table A-4 Data Results from dry ball milling testing

Tests							
IDENTIFICATION	Test 1	Test 2	Test 3	Test 4	Test 5	Test 6	
Temperature In (ºC)	16.1	14.2	14	13.9	12.8	13.5	
Temperature Out (ºC)	17.7	14.9	14.6	16.3	14.2	15.4	
Temperature Ambient (ºC)	17.9	15.3	14.4	15.8	14	15	
RPM	29.93	28.19	28.07	28.35	47.5	37.9	
Time (mm:ss)	5:00	3:00	5:00	10:00	5:00	5:00	
Current (A average)	4.968	4.832	4.971	4.694	6.204	5.054	
Average Size IN (μm)	3680	5180	5180	5180	5180	5180	
Total weight (g)	10948	9960	9979	9881	9994	9948	
6360-4000 (μm)	39	4724	3506	1683	1148	2211	
4000-3350 (μm)	1689	1502	1334	791	717	1042	
3350-2350 (μm)	2705	1205	1336	1057	1195	1324	
2350-1700 (μm)	1499	658	799	766	1045	931	
1700-800 (μm)	1540	622	869	1100	1562	1158	
800-600(μm)	636	242	377	648	788	545	
under 600 (μm)	2840	1007	1758	3836	3539	2737	
Balls							
BALL SIZE	DIAMETER (in)	VOL (in3)	VOLUME (m3)	TOTAL VOLUME (m3)	TOTAL WEIGHT (kg)	AMOUNT	AVG WEIGHT (kg)
1.5"	1.5	1.767	2.9E-05	8.109E-3	70.089	280	0.250
2.0"	2	4.189	6.86E-05	8.237E-3	70.33	120	0.586
Ball Mill							
	DIAMETER (m)	LENGTH (m)	VOLUME (m3)				
MILL	0.4318	0.6	8.7863E-2				

ANNEX H: DATA RESULTS FROM CHARPY HARDNESS TESTING

Table A-5 Data Results from Charpy Hardness Testing (not utilized).

ID	Long (mm)	Wide (mm)	Deep (mm)	Metered Delta (J)	Area (mm^2)	Delta J /A	Fraction from average
1	50.31	11.95	11.9	0.1	142.205	7.0321E-10	0.588
2	50.31	11.98	11.98	0	143.5204	0	0
3	50.81	12.06	12.11	0	146.0466	0	0
4	51.1	11.7	11.81	0.2	138.177	1.447E-09	0.954
5	52.18	11.72	12.06	0.2	141.3432	1.415E-09	0.928
6	63.1	25.2	18.8	0.2	473.76	4.222E-10	0.274
7	65.2	20.25	24.7	0.38	500.175	7.597E-10	0.440
8	60.75	19.1	24	0.3	458.4	6.545E-10	0.341
9	63.5	17.65	19.55	0.3	345.0575	8.694E-10	0.388
10	65	24	38.5	3.35	924	3.626E-09	1.345
11	68.95	40.25	24.4	1.75	982.1	1.782E-09	0.799
12	60.5	43.6	25.7	3	1120.52	2.677E-09	1

Variance	1.07E-18
Average	1.20E-09
Standard Deviation	1.03E-09

ANNEX I: IMAGES USED FOR SURFACE ENERGY CALCULATION

Figure A.8 Images used for Surface Energy calculation

ANNEX J: SOME OF THE IMAGES USED FOR IMAGE ANALYSIS.

INCOME AND OUTCOME MATERIAL ORE FROM UNIAXIAL TESTING.

Figure A.9 Some of the images used for image analysis. Photos of the income and outcome material from uniaxial testing